Vol. 637: 159–180, 2020
https://doi.org/10.3354/meps13240

MARINE ECOLOGY PROGRESS SERIES
Mar Ecol Prog Ser

Published March 5

Dissolved oxygen and temperature best predict deep-sea fish community structure in the Gulf of California with climate change implications

Natalya D. Gallo[1,2,*], Maryanne Beckwith[1], Chih-Lin Wei[3], Lisa A. Levin[1,2], Linda Kuhnz[4], James P. Barry[4]

[1]Integrative Oceanography Division, Scripps Institution of Oceanography, University of California San Diego, La Jolla, California 92093, USA

[2]Center for Marine Biodiversity and Conservation, Scripps Institution of Oceanography, University of California San Diego, La Jolla, California 92093, USA

[3]Institute of Oceanography, National Taiwan University, Taipei 106, Taiwan

[4]Monterey Bay Aquarium Research Institute, Moss Landing, California 95039, USA

ABSTRACT: Natural gradient systems can be used to examine the vulnerability of deep-sea communities to climate change. The Gulf of California presents an ideal system for examining relationships between faunal patterns and environmental conditions of deep-sea communities because deep-sea conditions change from warm and oxygen-rich in the north to cold and severely hypoxic in the south. The Monterey Bay Aquarium Research Institute (MBARI) remotely operated vehicle (ROV) 'Doc Ricketts' was used to conduct seafloor video transects at depths of ~200–1400 m in the northern, central, and southern Gulf. The community composition, density, and diversity of demersal fish assemblages were compared to environmental conditions. We tested the hypothesis that climate-relevant variables (temperature, oxygen, and primary production) have more explanatory power than static variables (latitude, depth, and benthic substrate) in explaining variation in fish community structure. Temperature best explained variance in density, while oxygen best explained variance in diversity and community composition. Both density and diversity declined with decreasing oxygen, but diversity declined at a higher oxygen threshold (~7 µmol kg^{-1}). Remarkably, high-density fish communities were observed living under suboxic conditions (<5 µmol kg^{-1}). Using an Earth systems global climate model forced under an RCP8.5 scenario, we found that by 2081–2100, the entire Gulf of California seafloor is expected to experience a mean temperature increase of 1.08 ± 1.07°C and modest deoxygenation. The projected changes in temperature and oxygen are expected to be accompanied by reduced diversity and related changes in deep-sea demersal fish communities.

KEY WORDS: Demersal fish · Deep-sea ecosystems · Hypoxia · Diversity · Gulf of California · Climate change · Community ecology · Oxygen minimum zone · ROV imaging

1. INTRODUCTION

Climate change is leading to warming ocean temperatures, decreasing pH, decreasing oxygen concentrations, and decreasing primary production (Bopp et al. 2013, Pörtner et al. 2014, Breitburg et al. 2018, IPCC 2019), including in the deep sea (Mora et al. 2013, Sweetman et al. 2017). Consequently, there is a critical need to understand organismal and ecosystem sensitivities to climate variables.

On continental margins, steep natural gradients in climate-relevant variables exist with depth. By sampling communities across spatial and vertical physicochemical gradients of interest, researchers can ex-

*Corresponding author: ndgallo@ucsd.edu

amine how environmental conditions correlate with differences in community patterns (Levin & Sibuet 2012, Gallo & Levin 2016). This approach, termed the natural laboratory approach, can also allow for the identification of important thresholds, both for community metrics and for individual species, which can later be tested using manipulative, controlled laboratory experiments and applied to predictive climate change models (Sperling et al. 2016).

The broad range of hydrographic conditions in the Gulf of California (hereafter referred to as the Gulf) make it an ideal study system to explore the relationship between climate variables and the structure of marine communities. Conditions change from a warm, oxygen-rich environment in the northern Gulf to cold and severely hypoxic in the southern Gulf. These regions decouple the relationship between environmental temperature, oxygen, and depth across relatively short latitudinal (~1126 km) and depth (~1400 m) ranges. In comparison, similar changes in environmental conditions do not occur even across a much larger latitudinal range from northern Washington State to the Pacific tip of Baja California.

Gulf ichthyofauna are composed of a mixture of northern and southern Eastern Pacific species, as well as a number of both widespread and endemic species (Walker 1960, Hastings et al. 2010). Several studies have described shallow-water and shelf fish communities (Walker 1960, Thomson & Eger 1966, Thomson et al. 2000, Hastings et al. 2010) as well as deep-sea midwater fish communities (Lavenberg & Fitch 1966, Robison 1972, Brewer 1973, De la Cruz-Agüero & Galván-Magaña 1992) in the Gulf. However, the ecology of the deep-sea demersal fish community remains virtually undescribed except in several valuable Spanish language references (López-Martínez et al. 2012, Del Moral-Flores et al. 2013, Mejía-Mercado et al. 2014, Zamorano et al. 2014).

Understanding how oceanographic conditions affect species distributions and community structure is a key goal of ecological studies, and is especially timely now that environmental conditions are rapidly changing due to human activities. In this study, we sought to differentiate the explanatory power of 'static' variables such as depth, latitude, and benthic substratum type from 'climate-relevant' variables such as temperature, oxygen, and primary production that are changing with climate (Bopp et al. 2013, Pörtner et al. 2014, IPCC 2019). If climate-relevant variables are highly correlated with existing community trends, then deep-sea communities may show strong responses to changing environmental conditions in the future.

Depth, latitude, temperature, oxygen, food input (i.e. primary production and carbon flux), and benthic habitat type all have the potential to influence the structure of deep-sea demersal fish communities in the Gulf. Hydrostatic pressure, directly related to depth, may explain depth zonation trends due to pressure adaptation limits across species (Carney 2005, Brown & Thatje 2014). However, temperature is considered by some to be most strongly associated with species zonation (Carney 2005), due in part to the strong influence of temperature on metabolic rates. Temperature and diversity may also be related, since warmer temperatures influence diversity by allowing a greater range of energetic lifestyles (Clarke & Gaston 2006). In the Barents Sea, temperature and depth were both found to be significant explanatory variables for trends in demersal fish density and diversity, with density positively related and diversity negatively related to temperature (Johannesen et al. 2012).

Oxygen minimum zones (OMZs) are known to influence the composition and diversity of demersal fish communities (Gallo & Levin 2016); however, research for the Gulf of California is limited. Along the west coast of the USA, demersal fish catch and species richness exhibited significant and positive relationships with near-bottom oxygen concentrations (Keller et al. 2015). Keller et al. (2017) observed an apparent threshold effect under hypoxic conditions, where small decreases in oxygen were associated with large decreases in total catch and species richness. Oxygen conditions found in the southern and central Gulf are extremely low and known to exclude most invertebrate species (Zamorano et al. 2007, Hendrickx & Serrano 2014). On average, demersal fish have been found to have higher oxygen requirements than benthic invertebrates (Vaquer-Sunyer & Duarte 2008), so we hypothesized that most demersal fish will be excluded from suboxic benthic environments (O_2 < 5 µmol kg^{-1}) in the Gulf, where the core of the OMZ intercepts the continental margin.

In this study, we made use of strong hydrographic differences in the Gulf to assess the relative power of environmental variables in explaining variation in the composition, density, and diversity of deep-sea demersal fishes. We hypothesized that 'climate-relevant' variables will have higher explanatory power than 'static' variables in explaining community trends. The objectives of this research were to (1) describe the bathymetric and latitudinal zonation of the deep-sea demersal fish community in the Gulf; (2) identify which environmental variables best explain variance in fish community composition, density, and diver-

sity, and identify threshold responses if they exist; (3) determine if demersal fish are absent from suboxic benthic habitats in the Gulf; and (4) consider the response of the fish community to future conditions projected by climate models for the Gulf.

2. MATERIALS AND METHODS

2.1. The Gulf of California

The Gulf of California exhibits some of the world's greatest environmental extremes, including large seasonal temperature fluctuations, a pronounced OMZ, and an extreme tidal range in the upper Gulf (Roden 1964, Álvarez-Borrego 1983). Large differences in temperature and oxygen between the north and south were first described in 1939 (Sverdrup 1941). Due to widespread upwelling of nutrient-rich water, the Gulf is also a very productive body of water (Espinosa-Carreón & Escobedo-Urías 2017). The oceanography of the Gulf has been extensively reviewed (Roden 1964, Álvarez-Borrego 2010) and is briefly described as it relates to this study.

Alluvial deposits from the Colorado River filled the northern Gulf, resulting in a relatively shallow, smooth concave seafloor (Moser et al. 1971). The Salsipuedes Basin (also known as the Ballenas Channel) is a deep basin in the northern Gulf. It is characterized by high temperatures, salinities, and oxygen at great depths due to mixing by strong tidal currents and isolation from the rest of the deep Gulf by a submarine ridge (Sverdrup 1941, Roden 1964, Álvarez-Borrego 1983). Due to the isolation of the Salsipuedes Basin, dramatic differences in temperature and oxygen are evident compared to the same depths south of the submarine ridge (Sverdrup 1941, Roden 1964).

The southern Gulf has one of the most extreme and thick OMZs in the world, with severely hypoxic conditions ($O_2 < 22.5$ µmol kg^{-1}) extending from shallower than 100 m to deeper than 1200 m. Conditions in the core of the OMZ, defined as the depth stratum within the OMZ where the lowest oxygen levels are observed, are nearly anoxic (Hendrickx & Serrano 2014).

2.2. Data collection

In 2015, the Monterey Bay Aquarium Research Institute (MBARI) Gulf of California research cruise on the R/V 'Western Flyer' used the remotely operated vehicle (ROV) 'Doc Ricketts' to conduct 8 dives at 5 locations to study benthic and demersal communities: Salsipuedes Basin, San Pedro Mártir Basin, Isla Tortuga, Cerralvo Trough, and Cabo Pulmo (listed north to south) (see Fig. 1, Table 1). The ROV

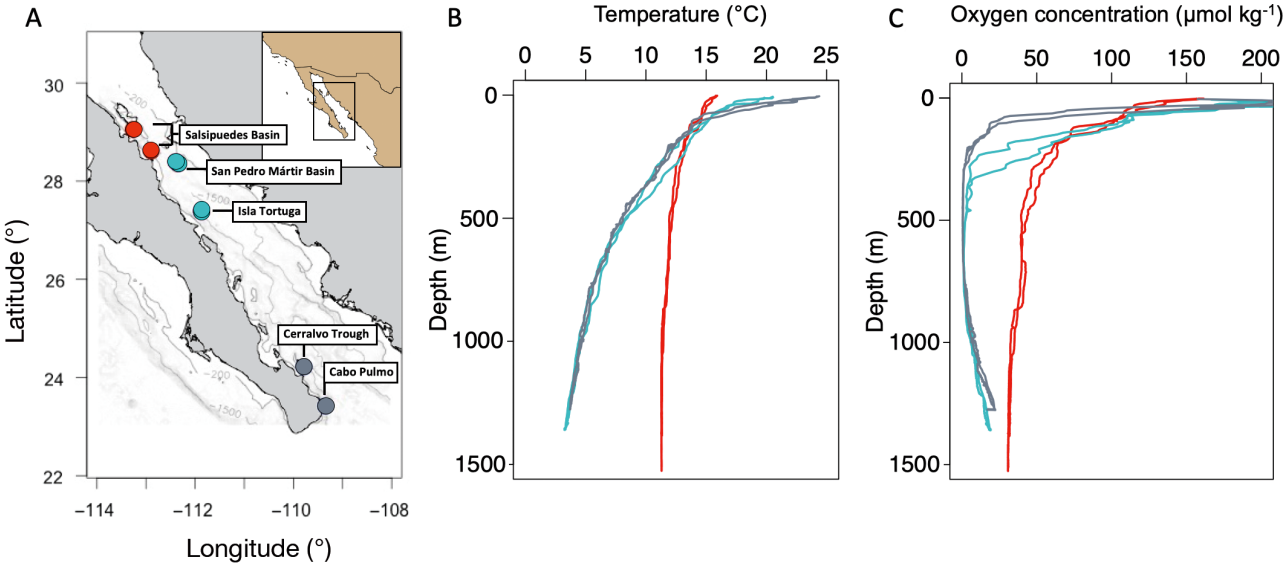

Fig. 1. (A) Locations of the 8 dives conducted with the remotely operated vehicle 'Doc Ricketts' in the Gulf of California. Inset: location of the Gulf of California relative to the US and Mexican Pacific coastline. Dive locations are indicated as points and color-coded by region (red: northern; turquoise: central; gray: southern). The 2 points in the central region represent 4 dives, but nearby locations make these independent dives difficult to see (Table 1). Dives were conducted upslope from depths of ~1400–200 m. The 200 and 1500 m isobaths for the Gulf of California are also shown. Representative water column profiles for (B) temperature and (C) oxygen are shown for Dives 733 (red, northern), 731 (turquoise, central), and 738 (gray, southern) to demonstrate differences in oceanographic conditions among the 3 regions

Table 1. Region, dive, date, location, annotated dive time (elapsed bottom time), number of fish transects, and environmental information for each of the 8 Gulf of California remotely operated vehicle dives analyzed in this study. Dives were conducted in the northern (N), central (C), and southern (S) Gulf of California; location coordinates correspond to the beginning of each dive. Environmental ranges represent minimum and maximum values encountered for each parameter during the total annotated dive period

Region/ Dive	Date	Location	Start latitude (°)	Start longitude (°)	Annotated dive time	No. of fish transects	Depth range (m)	Temperature range (°C)	Oxygen range (µmol kg^{-1})	Salinity range
C/731	21 Mar 15	Isla Tortuga	27.384269	−111.872958	4 h 20 min	7	1012–1358	3.28–4.58	6.48–18.96	34.55–34.59
C/732	22 Mar 15	Isla Tortuga	27.400906	−111.872560	9 h 01 min	12	200–952	4.70–12.96	1.22–40.18	34.54–34.88
N/733	23 Mar 15	Salsipuedes Basin	28.614186	−112.893840	2 h 16 min	0	737–1505	11.27–11.73	30.79–39.40	34.79–34.82
C/734	24 Mar 15	San Pedro Martir Basin	28.353634	−112.348216	8 h 05 min	12	200–919	6.19–12.98	1.30–29.01	34.54–34.87
N/735	25 Mar 15	Salsipuedes Basin	29.053637	−113.261312	10 h 33 min	10	196–1081	11.56–14.29	25.48–91.98	34.80–35.02
C/736	26 Mar 15	San Pedro Island North	28.395416	−112.392707	9 h 26 min	16	377–854	6.20–9.84	1.30–28.57	34.54–34.73
S/737	28 Mar 15	Cerralvo Trough	24.216883	−109.786416	6 h 29 min	10	295–959	4.80–11.14	0.52–6.22	34.50–34.72
S/738	29 Mar 15	Cabo Pulmo	23.419939	−109.348321	9 h 55 min	21	200–1274	3.72–12.12	0.39–21.96	34.48–34.78

was equipped with a suite of sensors (temperature, conductivity, pressure, transmissometer, fluorometer, oxygen optode, and Clark oxygen electrodes) that recorded continuously during all dives. High-definition video from the ROV was continuously recorded, including parallel lasers to provide a spatial scale in images. The video footage was annotated post-cruise using the Video Annotations and Reference System (VARS) (Schlining & Stout 2006). With the use of the ROV, 40 fish specimens were collected to aid in species identification of the fish species observed. Specimens were immediately frozen or preserved in either ethanol or formaldehyde and were identified by H. J. Walker at the Scripps Institution of Oceanography Pelagic Vertebrates Collection.

2.3. Species identification

Fish species observed in ROV images, as well as collected specimens, were identified using the following keys: Bradbury (1999) for ogcocephalids; Nielsen et al. (1999) for ophidiiformes; Springer (1979) for scyliorhinids; Walker & Rosenblatt (1988) for batrachoidids; and Fischer et al. (1995a,b) for other eastern tropical Pacific species. Although the identification of collected specimens was definitive, it is likely that some cryptic species observed only in video images may not have been identified correctly. Species richness from video analysis should thus be considered conservative, and the true number of unique species is likely somewhat higher. To reduce error in species annotations, species identifications were double-checked by 2 authors. All collected specimens were deposited in the Scripps Institution of Oceanography Vertebrates Collection. A master guide of all observed demersal fish species is provided in Supplement 1 at www.int-res.com/articles/suppl/m637p159_supp1.pdf, and images of fishes captured by the ROV are provided in Fig. S1 in Supplement 2 at www.int-res.com/articles/suppl/m637p159_supp2.pdf.

To confirm species identifications, collected specimens were sequenced for molecular identification. From each specimen that had been frozen or fixed in 95% ethanol, a section of underlying white muscle (~5–10 mg) was excised from the dorsal area. Ethanol-preserved samples were first washed several times with molecular-grade water to remove excess ethanol. A Chelex preparation was used to break down the tissues and release DNA (Walsh et al. 2013). This included adding 180 µl of a 10% Chelex solution to each tissue sample, vigorously vortexing the samples twice for 30 s, boiling samples at 100°C on a hot plate for 10 min, and then placing on ice. A 1 µl aliquot was collected from each extraction and used in a PCR reaction. The mitochondrial cytochrome oxidase *c* subunit 1 gene (CO1) and 16S ribosomal rRNA gene were amplified for molecular identification of collected specimens; primer sequences are provided in Text S1 in Supplement 2. Following amplification, an aliquot was run out on a gel, and the remaining PCR product was cleaned using a Sephadex G50 fine spin column and then quantified on a Nanodrop spectrophotometer. Samples

were sequenced by Retrogen. Recovered sequences were manually edited in Sequencher and compared to other sequences in NCBI GenBank using BLAST searches.

2.4. Transect design

Video footage (60 h) was collected during all dives and analyzed for fish observations. As the ROV transited upslope from depths of ~1400–200 m, standardized ~100 m long benthic transects were conducted for quantitative analyses of fish density, diversity, and community composition. Transects were not contiguous and were separated by ~100 m between transect lines. Parallel red lasers, 29 cm apart, illuminated images to indicate spatial scale. A total of 88 transects (~7–21 dive^{-1}) were conducted (Table 1). No quantitative transects were obtained during Dive 733 in the Salsipuedes Basin due to extremely strong current conditions and poor visibility, but noteworthy qualitative observations are reported. Median temperature, median oxygen, and median depth were reported for each transect and used for the analysis.

The area traversed for each transect was determined by its length (usually 100 m) and its width, which varied somewhat along each video transect. Transect length was determined by calculating the distance between the start and end coordinates of each transect, using the hypotenuse cumulative distance formula. For each transect, several screenshots were taken to represent the field of view for that transect. Screenshots were then used to calculate the horizontal field of view in ImageJ (National Institutes of Health) based on the known distance between laser points (29 cm). Field of view was averaged across all images for a given transect and multiplied by the distance traversed to calculate transect area. The average (±SD) horizontal field of view for all transects was 3.57 ± 0.72 m, and ranged between 2.31 and 6.37 m. Fish densities (fish m^{-2}) were calculated for all transects by dividing the number of fish observed in each transect by the area traversed. Fish were counted if they were within the image frame when they passed the lasers (midpoint of the frame), or if they were initially within the image frame but darted out in reaction to the ROV. However, fish behavioral avoidance or attraction to the ROV was rare, similar to other ROV studies (Ayma et al. 2016).

In addition to the environmental data collected by sensors on the ROV, an estimate of food input and benthic substrate type were determined for each transect. Benthic substrate type was determined by estimating the percentage of benthic surface covered by hard (e.g. rock) and soft (e.g. sand) substrate for each transect based on the ROV video. Food input for each transect was estimated in the following way. For each transect location, mean net primary productivity (NPP), seasonality of NPP, mean chlorophyll *a* (chl *a*) concentration, and euphotic depth were determined as in the supplemental information of Snelgrove et al. (2018). Export particulate organic carbon (POC) flux was then calculated using mean NPP, the seasonality of NPP, and export depth (ROV dive depth subtracting euphotic depth) according to Lutz et al. (2007). The average export POC flux was calculate for each transect with a search radius of 13 km over the gridded flux data (5 arc-minute resolution).

2.5. Data analysis and statistics

For each transect, fish community composition, density, and diversity were determined. Shannon-Wiener diversity ($H'_{\ln}$) was calculated as a metric of community diversity. We used SIMPER in the multivariate statistical analysis software package PRIMER v.6 (Clarke & Gorley 2006) to evaluate differences in community composition both within and between regions using a Bray-Curtis similarity matrix on square-root transformed fish count data. SIMPER was also used to assess contributions of specific taxa to community similarity across regions. ANOSIM in PRIMER v.6 was used to conduct pairwise tests of significance across regions. Dives were categorized as northern (Dives 733 and 735), central (Dives 731, 732, 734, and 736), or southern (Dives 737 and 738) in accordance with the biogeographic province regions identified by the Macrofauna Golfo project (Brusca & Hendrickx 2010, Hastings et al. 2010).

To visualize differences in community similarity and how these related to environmental variables, we used a non-metric multidimensional scaling (nMDS) ordination technique based on a Bray-Curtis dissimilarity matrix, using square-root transformed fish count data from each transect (n = 87), using the statistical package 'vegan' (Oksanen et al. 2017) in R v.3.6.0 (R Core Team 2019). To describe relationships between differences in community composition and environmental variables and test for breaks in community structure, we employed a multivariate regression tree (MRT) analysis (De'ath 2002) on square-root transformed fish count data from each transect (n = 87), using R packages 'mvpart' (De'ath 2014) and 'MVPARTwrap' (Ouellette & Legendre 2013). We included 7 environmental variables as predictors of

community structure: median temperature, median dissolved oxygen, median bottom depth, latitude, surface NPP, export POC flux, and percent hard substrate.

Generalized additive models (GAMs) (Hastie & Tibshirani 1986) were used to explore the relationship between environmental variables (median temperature, median dissolved oxygen, median bottom depth, latitude, surface NPP, export POC flux, and percent hard substrate) and the density (fish m^{-2}) and diversity (H'_{ln}) of demersal fish communities. Salinity only ranged between 34.5 and 35.0 and was not included in the model. To meet the assumptions of normality, density data were first log transformed. One transect with zero fish density was modified to 0.00001 fish m^{-2}. No transformation was used for diversity data. The R package 'mgcv' (Wood 2017) was used for the GAM analyses, and thin plate regression splines were used to fit the data, with latitude constrained to a maximum of 5 knots and NPP constrained to a maximum of 8 knots to prevent overfitting.

The same model structure was initially applied to both density and diversity data:

$$\text{Log(Density)} = s(\text{Latitude}, k = 5) + s(\text{Temperature}) + s(\text{Oxygen}) + s(\text{Depth}) + s(\text{POC flux}) + s(\%\ \text{Hard Substrate}) + s(\text{NPP}, k = 8)$$

$$\text{Shannon's } H'_{ln} = s(\text{Latitude}, k = 5) + s(\text{Temperature}) + s(\text{Oxygen}) + s(\text{Depth}) + s(\text{POC flux}) + s(\%\ \text{Hard Substrate}) + s(\text{NPP}, k = 8)$$

Since temperature and oxygen may also interact due to the effect of temperature on metabolism (Deutsch et al. 2015), we also tested a set of models that included a tensor product interaction term (ti) between temperature and oxygen. The model structure for these was:

$$\text{Log(Density)} = s(\text{Latitude}, k = 5) + ti(\text{Temperature}) + ti(\text{Oxygen}) + ti(\text{Temperature, Oxygen}) + s(\text{Depth}) + s(\text{POC flux}) + s(\%\ \text{Hard Substrate}) + s(\text{NPP}, k = 8)$$

$$\text{Shannon's } H'_{ln} = s(\text{Latitude}, k = 5) + ti(\text{Temperature}) + ti(\text{Oxygen}) + ti(\text{Temperature, Oxygen}) + s(\text{Depth}) + s(\text{POC flux}) + s(\%\ \text{Hard Substrate}) + s(\text{NPP}, k = 8)$$

Variables found to be non-significant ($p > 0.05$) were removed when model performance was improved following removal, and a suite of models was evaluated using the R Package 'MuMIn' (Bartoń 2019). Akaike's information criteria with correction for small sample size (AIC_C) and model weights were used to evaluate all models and select the most parsimonious one. Model fit was also evaluated through percent variance explained (R^2 adj) and generalized cross-validation (GCV). Component plots of the top-ranked models were visualized using the R package 'visreg' (Breheny & Burchett 2017). To identify variable importance, we tested the full suite of models including all variable combinations, both with and without a temperature–oxygen interaction, and then ranked variables by variable importance weights (Burnham & Anderson 2002) using the R package 'MuMIn.'

Since strong threshold responses for both density and diversity with oxygen concentration have previously been reported (Sperling et al. 2016, Keller et al. 2017), we used a broken-stick model in the R package 'segmented' (Muggeo 2008) to identify the presence of thresholds. Threshold responses were identified when an abrupt change in density or diversity was observed corresponding to a small change in oxygen concentration.

2.6. Climate model projections for the Gulf of California

To explore projections of benthic climate change, we used a fully coupled, 3-dimensional (3D) earth system model, Max Planck Institute's (MPI) ESM-MR (Giorgetta et al. 2013), to predict bottom temperature and dissolved oxygen levels under a concentration pathway RCP8.5 scenario representative of unchecked emissions growth. We chose MPI-ESM-MR because it has the highest spatial resolution (802 × 404) among all models within the Coupled Models Intercomparison Project Phase 5 (CMIP5) and therefore was suitable for our regional-scale analysis. All climate projection data were downloaded from the Earth System Grid Federation (ESGF) Peer-to-Peer (P2P) enterprise system (https://esgf-node.llnl.gov). Monthly projected temperatures were first averaged by year, and then yearly temperature and dissolved oxygen were averaged between 1951 and 2000 and between 2081 and 2100. We retained the bottom-most grids among the depth layers of decadal averages and then interpolated the raster layers to 10 arc-minute (approximately 0.167 arc-degree) grids by inverse distance weighting. The interpolated raster layers (georeferenced by latitude and longitude) were projected to cylindrical equal-area projection before cell statistics computation (e.g.

mean, SD). The geostatistical analyses used R packages 'raster' (Hijmans 2016), 'gstat' (Gräler et al. 2016), 'sp' (Bivand et al. 2013), and 'maptools' (Bivand & Lewin-Koh 2017).

3. RESULTS

3.1. Environmental differences between the northern, central, and southern Gulf of California

The oceanography of the Gulf varied dramatically between the northern and southern region. Profiles generated from the environmental sensors on the ROV (Fig. 1) showed that the stations at the southern end of the Gulf (Cabo Pulmo and Cerralvo Trough) were characterized by a thick and intense OMZ, where oxygen levels dropped below 22.5 µmol kg^{-1} by ~100 m depth and did not recover above these low levels until ~1250 m. In these locations the OMZ core, situated between 300 and 700 m, was nearly anoxic, with oxygen concentrations <1 µmol kg^{-1}. The lowest oxygen concentration encountered was 0.5 µmol kg^{-1} during dive 738 off Cabo Pulmo. Temperature decreased with depth and ranged from ~6–14°C in the OMZ. At the central Gulf stations, the OMZ (O_2 < 22.5 µmol kg^{-1}) began at deeper depths (~275 m) and extended deeper (~1400 m) than at southern stations. The OMZ core in the central Gulf was thinner (600–700 m), but still nearly anoxic (<1 µmol kg^{-1}). The temperature profile was similar to that of southern stations and the temperature range of the OMZ was ~3–12°C.

In contrast to the southern and central regions, the northern Gulf was characterized by a warmer, more oxygenated water column that was well-mixed due to strong tides that propagate through the narrow, deep Salsipuedes Basin. Profiles collected during the ROV dive showed a well-mixed water column below 250 m, with almost no change in oxygen or temperature between 250 and 1500 m (Fig. 1). Oxygen concentrations were >30 µmol kg^{-1} and temperatures were between 11 and 12°C across this depth range. At 1000 m, temperature was ~7°C warmer and oxygen was ~26 µmol kg^{-1} higher in the northern Gulf than at similar depths in the central and southern Gulf.

Productivity patterns also varied across the Gulf, with the northern Gulf characterized by higher mean NPP, higher mean chl *a*, higher export POC flux, and a shallower euphotic depth than the southern Gulf; the central Gulf had intermediate conditions. A higher proportion of hard substrate was also observed during transects in the northern and central Gulf than in the southern Gulf. Differences in environmental conditions across all transects are visualized in Fig. S2 in Supplement 2.

3.2. The deep-sea demersal fish community

A total of 48 demersal fish species were observed during the ROV dives (Table 2, Supplement 1). However, this number is likely conservative as cryptic species may have been present that are indistinguishable using ROV video footage alone. For example, several deep-water macrourid species were grouped as Macrouridae due to the difficulty of distinguishing grenadier species in the ROV video footage. These include *Coryphaenoides capito* and *Nezumia liolepis*, and may include *N. convergens* and *C. anguliceps* (Zamorano et al. 2014).

With the use of the ROV manipulator arm and suction hose, 40 fish specimens were collected. Based on the morphological and genetic information, we were able to confirm that these represented 20 distinct species (Table 2). We were able to successfully sequence 70% of the species collected (14/20) for mitochondrial CO1 gene, but only 30% (6/20) for 16S ribosomal rRNA gene (16S). We were consistently unable to sequence the collected macrourids for either CO1 or 16S: specimens of all 3 macrourid species (*N. liolepis*, *C. capito*, *Coelorinchus scaphopsis*) failed to amplify in the PCR reaction. All high-quality sequences were deposited in GenBank (MN022242–MN022262).

3.2.1. Northern Gulf of California

High current conditions encountered during Dive 733 in the Salsipuedes Basin allowed only qualitative observations. The community observed on this dive was composed of *Sebastes cortezi*, *Eptatretus sinus*, *Parmaturus xaniurus*, and *Hydrolagus colliei*. *S. cortezi* was observed here at depths deeper than expected (1126–1448 m).

Quantitative transects for the northern region were restricted to Dive 735. At the shallowest depths (200–400 m), the fish community was dominated by *C. scaphopsis* (~48%), *Pontinus furcirhinus* (~22%) (Fig. 2A), and *Physiculus rastrelliger* (9%). Several species were observed across a broad depth range: *E. sinus* (390–1080 m), *Sebastes* spp. (242–1009 m) including *S. cortezi* and *S. exsul*, and *Symphurus* spp. (289–1010 m) including *S. oligomerus* (Table 2). Shallower than 786 m, the macrourid *C. scaphopsis*

Table 2. Demersal fish species observed during remotely operated vehicle dives, along with the dive identification numbers and observed environmental conditions. Entries in gray represent collected specimens that were identified in the lab and sequenced

Species	Dive number	Depth range (m)	Temp. range (°C)	Oxygen range (µmol kg^{-1})
Bathycongrus macrurus	732, 737, 738	298–544	7.32–11.61	0.65–12.19
Bathypterois sp.	731, 732, 737, 738	863–1356	3.32–5.07	4.12–21.74
Cataetyx rubrirostris	738	1253	3.78	20.31
Cephalurus cephalus	732, 734, 736, 737, 738	494–918	5.34–8.11	0.83–3.17
Cephalurus cephalus	732	716	6.17	1.6
Cherublemma emmelas	732, 734, 736, 737, 738	325–955	4.71–10.46	0.52–7.33
Cherublemma emmelas	732	577	7.31	1.52
Cherublemma emmelas	736	798	6.43	1.43
Cherublemma emmelas	737	853	5.13	4.08
Chilara taylori	732, 734	208–306	11.74–12.90	14.06–27.68
Coelorinchus scaphopsis	734, 735, 736	222–786	9.53–13.20	20.78–60.92
Coelorinchus scaphopsis	734	382	10.65	22.99
Coelorinchus scaphopsis	735	296	12.97	55.67
Coryphaenoides capito	732	921	5.02	4.08
Cottoidea sp.	732	203–260	12.74–12.96	31.89–39.70
Derepodichthys alepidotus	738	1182	3.98	16.57
Dibranchus spp.	731, 732, 737, 738	733–1271	3.66–6.11	1.61–21.74
Dibranchus hystrix	732	922	5.02	3.99
Dibranchus hystrix	737	946	4.81	6.09
Dibranchus hystrix	738	1184	3.96	16.75
Dibranchus spinosus	732, 737, 738	723–1243	3.83–6.06	1.30–19.44
Dibranchus spinosus	738	1126	4.31	11.63
Eknomoliparis chirichignoae	731	1314	3.51	16.4
Eptatretus sinus	732, 733, 734, 735, 736, 737	263–1080	5.01–12.08	2.73–35.02
Eretmichthys pinnatus	731, 737, 738	867–1264	3.74–5.06	4.25–21.39
Gnathophis cinctus	735	285–302	13.16–13.44	60.05–67.47
Gnathophis cinctus	735	285	13.44	67.47
Hydrolagus colliei	733, 735, 736	369–1020	9.50–13.11	19.74–58.62
Lestidiops sp.	732	294	11.87	17.09
Liopropoma longilepis	732, 735	199–261	12.81–13.82	29.42–79.10
Lophiodes caulinaris	732, 734, 735, 738	217–888	10.54–12.07	2.99–29.46
Lycenchelys sp. 1	731, 732, 737, 738	894–1355	3.31–4.88	5.55–21.00
Lycenchelys sp.	738	1184	3.99	16.4
Lycenchelys sp. 2	731, 732, 737, 738	898–1355	3.32–5.03	4.03–21.91
Lycenchelys sp. 2	737	946	4.8	6.07
Macrouridae spp.	731, 732, 734, 735, 736, 737, 738	460–1355	3.33–11.64	0.82–29.94
Merluccius sp.	732, 736	339–457	8.16–11.51	5.29–28.51
Nemichthys sp.	737	411	9.57	0.87
Nettastomatidae sp.	738	1227–1254	3.78–3.87	18.70–20.65
Nezumia liolepis	738	934	4.79	6.51
Opichthus frontalis	735	681	11.81	31.24
Paralabrax auroguttatus	735	217	13.78	76.37
Paraliparis rosaceus	731, 738	935–1348	3.37–4.77	6.51–17.79
Paraliparis rosaceus	738	935	4.77	6.51
Parmaturus xaniurus	733, 734, 735, 736, 738	377–1173	4.11–11.59	1.43–26.60
Parmaturus xaniurus	736	798	6.44	1.43
Physiculus rastrelliger	732, 734, 735, 736, 738	216–483	8.33–13.49	1.08–68.95
Physiculus rastrelliger	732	443	9.08	3.12
Physiculus rastrelliger	735	392	12.09	35.28
Pontinus furcirhinus	732, 734, 735	197–387	10.44–13.86	6.42–79.36
Pontinus furcirhinus	734	333	11.12	24.82
Pontinus sierra	737, 738	202–301	11.05–12.11	1.82–5.08
Pontinus sierra	737	301	11.05	1.82
Porichthys mimeticus	737, 738	223–229	11.56–11.82	3.08–3.69
Porichthys mimeticus	737	250	11.56	3.08
Pronotogrammus eos	734	203–213	12.85–12.88	27.59–27.73
Raja sp. 1	735, 736	300–511	11.99–12.90	33.28–53.32
Raja sp. 2	735	276	13.17	60.79
Sebastes cortezi	733, 734, 735, 736	199–1448	7.26–14.26	1.82–91.12
Sebastes cortezi	736	559	7.65	2.48
Sebastes exsul	735	199–662	11.83–13.86	31.15–79.67
Sebastes macdonaldi	734	232–287	11.98–12.68	26.82–27.34
Serranidae sp.	738	223–227	11.79–11.81	3.21–3.47
Squatinidae sp.	735	291	13.12	59.23
Symphurus spp.	732, 734, 735, 736	224–1010	7.89–12.98	2.69–55.28
Symphurus oligomerus	735	808	11.67	30.33
Synodus sp.	738	212	11.83	3.56
Triglidae sp.	732	264	12.76	33.76
Xeneretmus ritteri	734	383	9.78	13.88
Zoarcidae sp.	731, 738	1160–1348	3.37–4.13	10.07–19.61

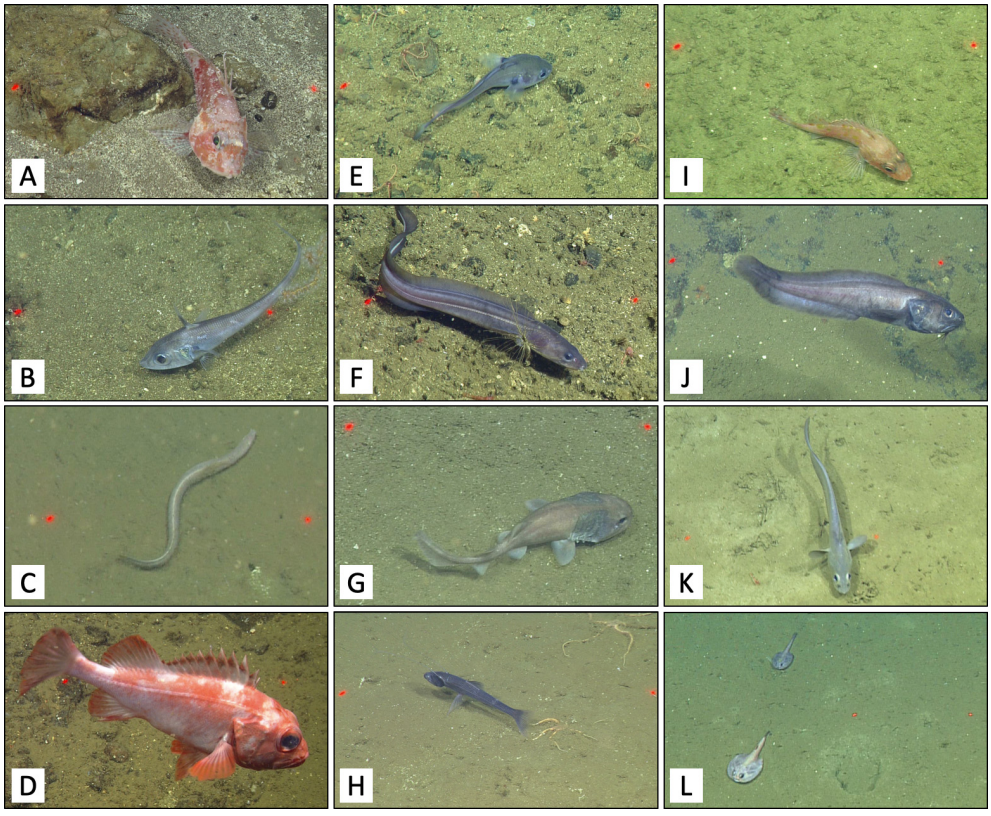

Fig. 2. Common deep-sea demersal fish species in the (A–D) northern, (E–H) central, and (I–L) southern Gulf of California. (A,E,I) Species commonly found from 200–400 m; (B,F,J) from 400–700 m, (C,G,K) from 700–1000 m, and (D,H,L) deeper than 1000 m. (A) *Pontinus furcirhinus*; (B) *Coelorinchus scaphopsis*; (C) *Eptatretus sinus*; (D) *Sebastes cortezi*; (E) *Physiculus rastrelliger*; (F) *Bathycongrus macrurus*; (G) *Cephalurus cephalus*; (H) *Bathypterois pectinatus*; (I) *Pontinus sierra*; (J) *Cherublemma emmelas*; (K) *Coryphaenoides capito*; (L) *Dibranchus spinosus* (lower left) and *Dibranchus hystrix* (upper middle). A variety of species were selected to give a visual representation of the different species observed in the Gulf. Most of the pictured species were not restricted to only the region or depth range indicated in this figure, but are shown where they were encountered frequently. Lasers (red dots) are provided for scale in each image; distance between lasers: 29 cm

was common in open sandy areas (~50% community composition) (Fig. 2B). Similar to Dive 733, the deep-water community (>700 m) here was characterized by *E. sinus* (Fig. 2C), *S. cortezi* (Fig. 2D), *P. xaniurus*, and *H. colliei*. Rare species observed during this dive included *Paralabrax auroguttatus*, *Gnathophis cinctus*, *Ophichthus frontalis*, and others shown in Table 2.

3.2.2. Central Gulf of California

A total of 4 dives (731, 732, 734, and 736) in 2 locations, near Isla Tortuga and San Pedro Island, were used to characterize the central Gulf deep-sea demersal fish community. Unlike the northern Gulf, *E. sinus* was absent in deep water, but present shallower (<500 m). *P. rastrelliger* (~18%) (Fig. 2E), *P. furcirhinus* (~16%), *Sebastes* spp. (~15%), *E. sinus* (~15%), and *Bathycongrus macrurus* (~10%) (Fig. 2F) dominated the fish community shallower than 500 m. At intermediate depths (600–1000 m), the central community was dominated by *Cherublemma emmelas* (~43%) and *Cephalurus cephalus* (~40%) (Fig. 2G). The deep-water community (>1000 m) was dominated by *Bathypterois* sp. (41%) (Fig. 2H), Macrouridae (36%), and *Lycenchelys* spp. (10%). Rarer species (<10%) included *Dibranchus* spp., *Eknomoliparis chirichignoae*, *Paraliparis rosaceus*, *Liopropoma longilepis*, *Sebastes macdonaldi*, *Xeneretmus ritteri*, *Chilara taylori*, and others (Table 2). A previous record of *C. taylori* from the Gulf was considered doubtful (Nielsen et al. 1999), but the 3 observations of *C. taylori* confirm that this species' range extends into the central Gulf.

We observed noteworthy differences in the fish communities in the central region. During Dive 734, *C. scaphopsis* were common members (~36%) of the shallow (200–400 m) community, but rare (< 5%) during Dive 736, and absent in the more southern Dives 731 and 732. There may be a latitudinal break in the

distribution of *C. scaphopsis* between 27°–28° N. Dive 736 also differed from other dives in the central region with a high abundance of *E. sinus* (~36%), *Sebastes* spp. (~31%), *P. xaniurus* (~11%), and *H. colliei* (~7%) observed in shallower areas (300–400 m). Differences in community composition may be influenced by the contrasting benthic habitat, primarily a boulder field, that dominated Dive 736.

While *Sebastes* spp. are thought to be relatively intolerant of hypoxia (McClatchie et al. 2010), *S. cortezi* was observed living in deep-water areas under severely hypoxic conditions (1.83–7.61 µmol kg^{-1}) in the central Gulf. To our knowledge, these represent the lowest oxygen records for a rockfish species.

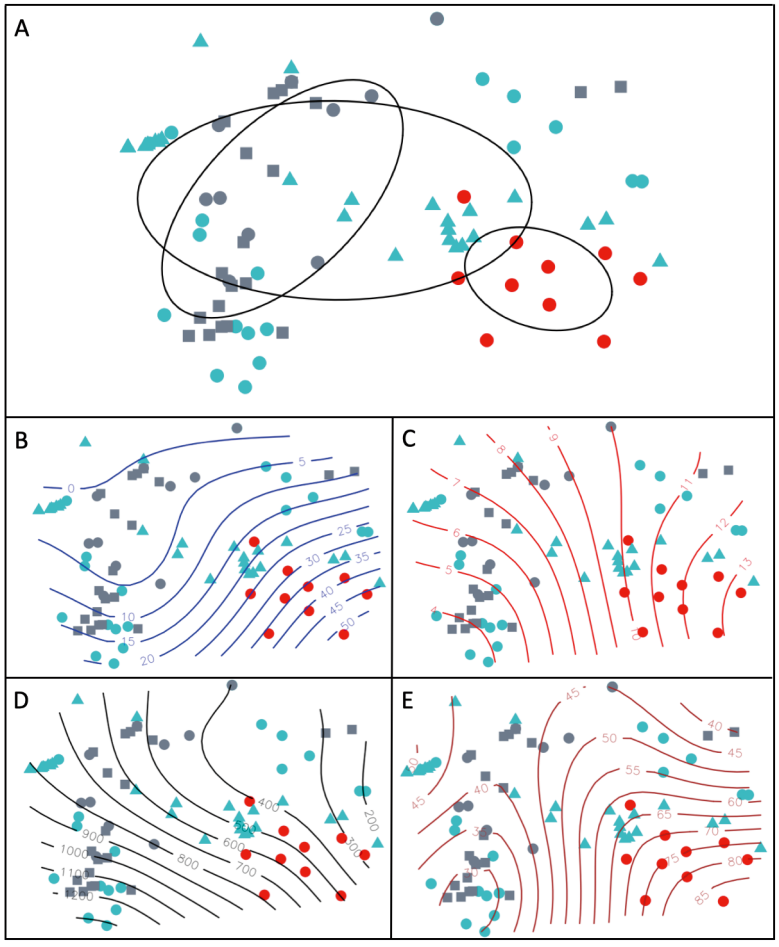

Fig. 3. Multidimensional scaling plot of Bray-Curtis similarity matrix based on square-root transformed fish abundance data (2D stress: 0.08). Each point represents the fish assemblage and counts in a ~100 m long transect; colors indicate transects from the northern (red), central (turquoise), and southern (gray) Gulf of California. Dives from different locations are differentiated by shape: red circles: transects from Dive 735 in the Salsipuedes Basin; turquoise circles: Dives 731 and 732 off Isla Tortuga; turquoise triangles: Dives 734 and 736 off Isla San Martir; gray circles: Dive 737 off Isla Cerralvo; and gray squares: Dive 738 off Cabo Pulmo. (A) Ellipses represent grouping by region with 50% confidence limits. Non-metric multidimensional scaling plots are shown with overlain environmental contours that indicate (B) oxygen concentration (µmol kg^{-1}), (C) temperature (°C), (D) depth (m), and (E) export particulate organic carbon flux (mg C m^{-2} d^{-1})

3.2.3. Southern Gulf of California

Dives 737 and 738 in the Cerralvo Trough and off Cabo Pulmo were used to characterize the southern Gulf deep-sea demersal fish community. Shallower than 400 m, this community was dominated by *B. macrurus* (38%), *Porichthys mimeticus* (23%), and *Pontinus sierra* (~15%) (Fig. 2I). *C. scaphopsis*, a very common member of the shallow-water community at the more northern sites, was completely absent in the south. Similarly, *Sebastes* spp. were completely absent in the south. Between 400 and 900 m, *C. emmelas* dominated the fish community (63%) (Fig. 2J), and co-occurred with Macrouridae (~19%) and *Dibranchus spinosus* (~6%) within the deeper portion of its depth range (700–900 m). Myctophids and bathylagids were observed swimming near or crashing into the seafloor at depths between 400 and 700 m. Similar to the central Gulf, the deep-water community (>1000 m) in the southern Gulf was dominated by Macrouridae (29%) (Fig. 2K), *Bathypterois* sp. (~26%), and *Lycenchelys* spp. (16%). Rarer species included *Dibranchus* spp. (10%) (Fig. 2L), *Eretmichthys pinnatus* (8%), and *D. spinosus* (6%).

3.2.4. Community similarity in the northern, central, and southern Gulf

Demersal fish communities differed significantly among the northern, central, and southern Gulf regions (ANOSIM, Global R = 0.17, $p < 0.01$; Fig. 3) and between each regional pair (ANOSIM, $p < 0.01$). The northern assemblages grouped together and were entirely distinct from southern assemblages. Overall, the central Gulf fish community was the most heterogeneous, with elements of both northern and southern communities under similar environmental conditions (Fig. 3). Assemblages in the south-

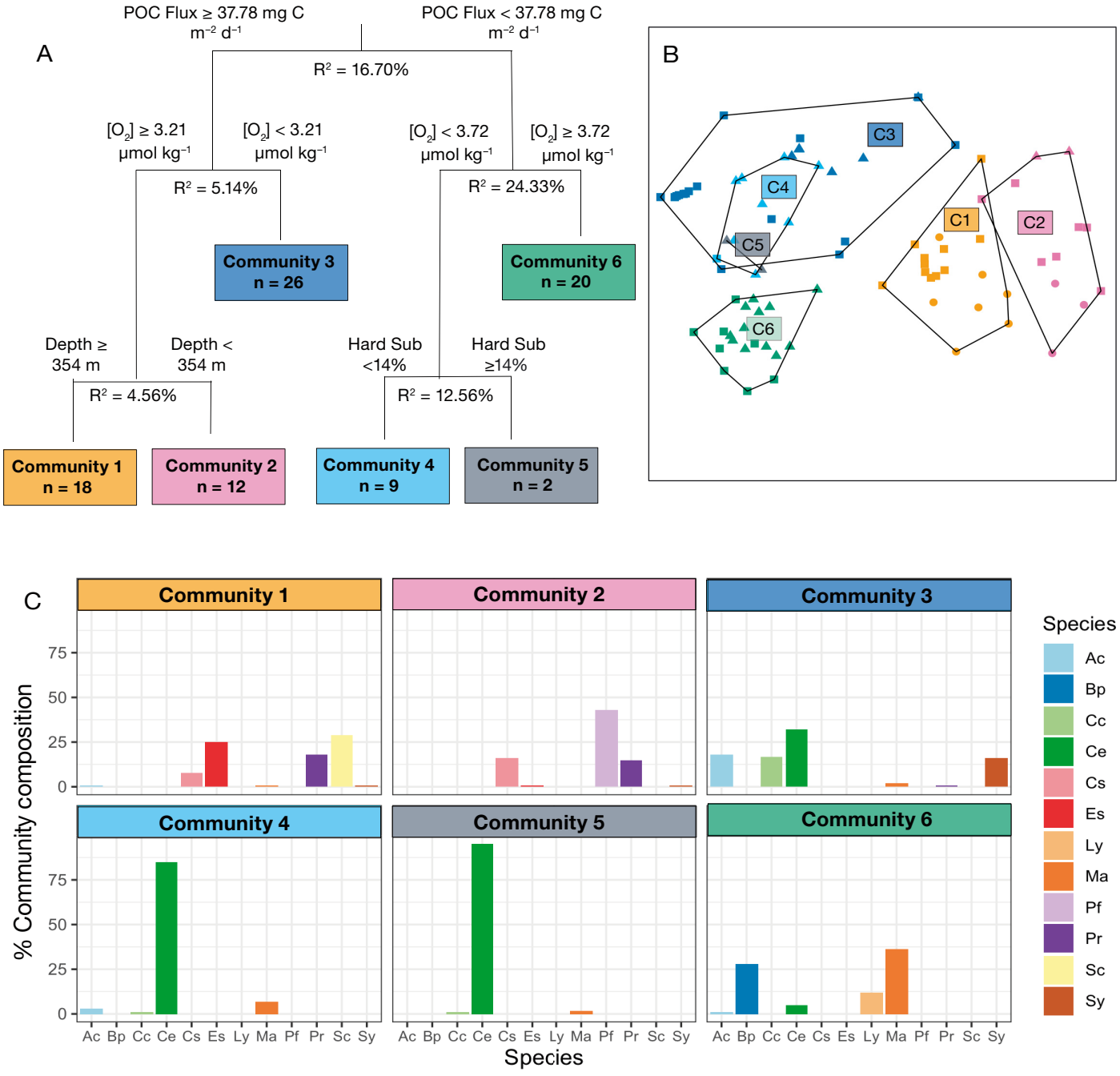

Fig. 4. Gulf of California deep-sea demersal fish community composition as a function of environmental covariates based on a multivariate regression tree (MRT) analysis. (A) MRT for the selected model which explains 63 % of the variance in community composition with 4 covariates (particulate organic carbon [POC] flux, oxygen concentration, depth, and % hard substrate) (RE = 0.367, CV Error = 0.721, SE = 0.25). The tree shows each split, the variance explained (R^2) by each split, the 6 unique communities identified, and the number of samples that were representative of each community. (B) Multidimensional scaling plot of Bray-Curtis similarity matrix based on square-root transformed fish count data (2D stress: 0.08) color-coded by community groups identified by the MRT analysis. Colors correspond to the colors in (A) for each community and convex hulls are drawn to demarcate each community. Shapes indicate transects from the northern (circles), central (squares), and southern (triangles) Gulf of California. (C) Relative community composition for each distinct community identified by the MRT analysis. Only 11 dominant species that made up ≥10 % of the community composition for any of the 6 communities are shown, but these 11 species comprise 76–98 % of the 6 communities. Species names are abbreviated as follows: Ac: Actinopterygii; Bp: *Bathypterois pectinatus*; Cc: *Cephalurus cephalus*; Ce: *Cherublemma emmelas*; Cs: *Coelorinchus scaphopsis*; Es: *Eptatretus* sp.; Ly: *Lycenchelys* spp.; Ma: Macrouridae; Pf: *Pontinus furcirhinus*; Pr: *Physiculus rastrelliger*; Sc: *Sebastes cortezi*; and Sy: *Symphurus* spp.

ern Gulf also showed high heterogeneity, though they were more homogeneous than assemblages in the central Gulf (Fig. 3).

Using SIMPER, we found that community similarity was highest (35%) for the northern Gulf, lowest (15%) for the central Gulf, and intermediate for the southern Gulf (27%). For the northern sites, *S. cortezi* and *C. scaphopsis* contributed the most (79%) to community similarity. *C. emmelas* and Macrouridae contributed the most to community similarity (55%) for the southern region. Southern and northern demersal fish communities had very high average dissimilarity (99%) and only shared 3 species: *E. sinus*, *Lophiodes caulinaris*, and *P. rastrelliger*. Average dissimilarity between northern and central communities was 89%, similar to the dissimilarity between central and southern communities (88%). The species that contributed the greatest to the dissimilarity between northern and central sites were *C. scaphopsis* and *S. cortezi*, which were both more abundant in the northern Gulf. The species that contributed the greatest to the dissimilarity between the central and southern sites were *C. emmelas* and Macrouridae, which were more abundant in the southern transects.

3.3. Relationship between environmental variables and demersal fish community composition, density, and diversity

For the MRT analysis, the selected tree identified export POC flux, oxygen concentration, depth, and percent hard substrate as primary drivers explaining community transition points (Fig. 4). The tree with the smallest cross-validation relative error (CVRE = 0.654, RE = 0.198) included 17 splits, and the most parsimonious tree, which was within 1 standard error of the smallest CVRE value, included 3 splits. We selected a tree that was intermediate between these 2, which contained 5 splits and 6 leaves (i.e. communities) (Fig. 4), and explained ~63% of the variance in community composition (CVRE = 0.721, RE = 0.367). An oxygen concentration of ~3.5 µmol kg^{-1} was identified as an important transition point at 2 splits in the tree and explained ~29% of the variance in community composition. Communities 1 and 2 were present under higher oxygen conditions and differed by depth, with *S. cortezi* and *Eptatretus* sp. most common in the deeper community (C1) and *P. furcirhinus* most common in the shallower community (C2). Communities 3, 4, and 5 were present under lower oxygen conditions; these all had high representation of *C. emmelas* and overlapped in the nMDS (Fig. 4B). However, Community 3 had a more even community composition, whereas Communities 4 and 5 were characterized by very high dominance of *C. emmelas* (Fig. 4C). Community 6 was distinct from all other communities (Fig. 4B), was characterized by high representation of Macrouridae and *Bathypterois pectinatus* (Fig. 4C), and was present under higher oxygen conditions but lower POC flux (Fig. 4A).

In addition to exploring how community composition correlated with environmental conditions, we also examined if environmental conditions explained trends in fish community density and diversity. Using GAMs, we found that fish density and diversity exhibited differing responses.

GAMs including a suite of environmental factors explained up to 75% of the variation in fish community density. The top-ranked model included temperature, oxygen concentration, an interaction between temperature and oxygen, latitude, mean NPP, depth, and percent hard substrate as covariates (Table 3). Export POC flux was the only covariate that did not improve model performance. Models that included a temperature–oxygen interaction were ranked consistently higher than others (Table 3) and the 2D component plot showed that fish density increased with higher temperature and higher oxygen conditions, but decreased under warmer temperatures (>9.5°C) under suboxic conditions (O_2 < 5 µmol kg^{-1}) (Fig. 5). Depth and latitude both had a negative relationship with density, with fish density decreasing at deeper depths and at higher latitudes. In contrast, fish density increased with mean NPP and percent hard substrate. When considering combinations of covariates for models that included a temperature–oxygen interaction, the following variables were ranked as most important for explaining variance in fish density: temperature, the interaction between temperature and oxygen, latitude, mean NPP, depth, percent hard substrate, POC flux, and oxygen. If a temperature–oxygen interaction was excluded, then oxygen and temperature were ranked as the most important covariates.

While fish density was affected by a number of covariates (Fig. 5), the top-ranked model for fish community diversity only included oxygen and latitude (Table 4) and accounted for 57% of the variance in fish community diversity. Diversity showed a strong threshold response to environmental oxygen, with diversity decreasing sharply once oxygen levels became too low (Fig. 6), and exhibited a nonlinear relationship with latitude, with lower diversity at mid latitudes in the Gulf (Fig. 6). Unlike for density, the top model for fish diversity did not include a temperature–oxygen interaction, and temperature,

Table 3. Generalized additive models evaluated for assessing the relationship between environmental variables and demersal fish density across 88 transects in the Gulf of California. Models included latitude (Lat), near-bottom temperature (T), near-bottom dissolved oxygen (Ox), depth (Z), export particulate organic carbon flux (POC), percent hard substrate (Sub), and mean net primary production (NPP) as explanatory variables. Certain models also included an interaction between temperature and oxygen (T,Ox). Models are ordered based on model performance evaluated by Akaike's information criteria with correction for small sample size (AIC_C), with the most parsimonious model ($\Delta AIC_C = 0$) at the top. Model weight (Weight), generalized cross-validation (GCV), variance explained (R^2 adj), and significance (p-value) of each covariate included in the model are also shown. Covariates that were significant ($p < 0.05$) are indicated in **bold**. N/A: not applicable (covariates not included in the model)

Equation	AIC_C	ΔAIC_C	Weight	GCV	R^2 (adj)	p							
						Lat	T	Ox	T,Ox	Z	POC	Sub	NPP
Log(Density) = s(Lat) + ti(T) + ti(Ox) + ti(T,Ox) + s(Z) + s(Sub) + s(NPP)	258.73	0	0.781	0.842	0.749	**<0.001**	**<0.001**	**0.016**	**<0.001**	**<0.001**	N/A	**0.016**	**<0.001**
Log(Density) = s(Lat) + ti(T) + ti(Ox) + ti(T,Ox) + s(Z) + s(NPP)	263.21	4.48	0.083	0.895	0.731	**0.003**	**0.003**	**0.022**	**<0.001**	**0.001**	N/A	N/A	**<0.001**
Log(Density) = s(Lat) + ti(T) + ti(Ox) + ti(T,Ox) + s(Z)	264.57	5.84	0.042	1.058	0.626	**<0.001**	**0.001**	**<0.001**	**<0.001**	**0.003**	N/A	N/A	N/A
Log(Density) = s(Lat) + ti(T) + ti(Ox) + ti(T,Ox) + s(NPP)	264.91	6.18	0.036	0.978	0.687	0.076	**<0.001**	0.613	**<0.001**	N/A	N/A	N/A	**<0.001**
Log(Density) = ti(T) + ti(Ox) + ti(T,Ox) + s(NPP)	265.26	6.53	0.03	0.979	0.687	N/A	**<0.001**	0.527	**<0.001**	N/A	N/A	N/A	**<0.001**
Log(Density) = s(Lat) + ti(T) + ti(Ox) + ti(T,Ox) + s(Z) + s(POC) + s(NPP)	267.57	8.84	0.009	1.049	0.649	0.054	**0.018**	0.108	**<0.001**	**<0.001**	0.861	N/A	0.068
Log(Density) = s(Lat) + s(T) + s(Ox)	268.03	9.3	0.007	1.125	0.588	**<0.001**	**<0.001**	**<0.001**	N/A	N/A	N/A	N/A	N/A
Log(Density) = s(Lat) + s(T) + s(Ox) + s(NPP)	269.1	10.37	0.004	1.113	0.606	0.105	**<0.001**	**<0.001**	N/A	N/A	N/A	N/A	**<0.001**
Log(Density) = s(Lat) + s(T) + s(Ox) + s(Z)	270.79	12.06	0.002	1.151	0.584	**<0.001**	**<0.001**	**<0.001**	N/A	0.910	N/A	N/A	N/A
Log(Density) = s(Lat) + ti(T) + ti(Ox) + ti(T,Ox) + s(Z) + s(POC) + s(Sub) + s(NPP)	271.27	12.54	0.001	0.885	0.754	**0.003**	0.053	**0.006**	**<0.001**	**<0.001**	0.068	**0.003**	**<0.001**
Log(Density) = s(T) + s(Ox) + s(NPP)	271.91	13.18	0.001	1.120	0.618	N/A	**<0.001**	**<0.001**	N/A	N/A	N/A	N/A	**<0.001**
Log(Density) = s(Lat) + s(T) + s(Ox) + s(Z) + s(NPP)	271.98	13.25	0.001	1.138	0.604	0.095	**<0.001**	**<0.001**	N/A	0.800	N/A	N/A	**0.002**
Log(Density) = s(Lat) + ti(T) + ti(Ox) + ti(T,Ox)	272.81	14.08	0.001	1.190	0.563	**<0.001**	**0.035**	**<0.001**	**<0.001**	N/A	N/A	N/A	N/A
Log(Density) = s(Lat) + s(T) + s(Ox) + s(Z) + s(POC) + s(NPP)	275.14	16.41	0	1.169	0.598	0.199	**<0.001**	**<0.001**	N/A	0.857	0.919	N/A	**0.023**
Log(Density) = s(Lat) + s(T) + s(Ox) + s(Z) + s(Sub) + s(NPP)	275.36	16.63	0	1.171	0.598	0.098	**<0.001**	**<0.001**	N/A	0.770	N/A	0.639	**0.002**
Log(Density) = s(Lat) + s(T) + s(Ox) + s(Z) + s(POC) + s(Sub) + s(NPP)	278.61	19.89	0	1.203	0.592	0.200	**<0.001**	**<0.001**	N/A	0.854	0.929	0.633	**0.020**
Log(Density) = s(T) + s(NPP)	293.7	34.97	0	1.570	0.371	N/A	**<0.001**	N/A	N/A	N/A	N/A	N/A	**0.009**
Log(Density) = s(Lat) + s(T)	294.94	36.21	0	1.586	0.371	**0.045**	**<0.001**	N/A	N/A	N/A	N/A	N/A	N/A
Log(Density) = s(T) + s(Ox) + s(Z)	295.35	36.62	0	1.581	0.385	N/A	**<0.001**	0.154	N/A	**0.021**	N/A	N/A	N/A
Log(Density) = s(Lat) + s(T) + s(Z)	296.78	38.05	0	1.614	0.366	0.276	**<0.001**	N/A	N/A	0.329	N/A	N/A	N/A
Log(Density) = s(T) + s(Ox)	297.86	39.13	0	1.626	0.368	N/A	**<0.001**	**0.163**	N/A	N/A	N/A	N/A	N/A
Log(Density) = s(Lat) + s(Ox) + s(Z)	298.38	39.65	0	1.596	0.410	**<0.001**	N/A	**<0.001**	N/A	**<0.001**	N/A	N/A	N/A
Log(Density) = s(T)	298.98	40.25	0	1.675	0.320	N/A	**<0.001**	N/A	N/A	N/A	N/A	N/A	N/A
Log(Density) = ti(T) + ti(Ox) + ti(T,Ox)	299.36	40.63	0	1.577	0.439	N/A	**<0.001**	0.402	**<0.001**	N/A	N/A	N/A	N/A
Log(Density) = ti(T) + ti(Ox) + ti(T,Ox) + s(Z)	300.07	41.34	0	1.618	0.408	N/A	**<0.001**	**0.030**	**<0.001**	**0.035**	N/A	N/A	N/A
Log(Density) = s(Lat) + s(Ox)	308.33	49.6	0	1.890	0.187	**<0.001**	N/A	**0.001**	N/A	N/A	N/A	N/A	N/A
Log(Density) = s(Ox) + s(NPP)	309.01	50.28	0	1.909	0.166	N/A	N/A	**<0.001**	N/A	N/A	N/A	N/A	**<0.001**
Log(Density) = s(POC)	313.91	55.18	0	1.987	0.190	N/A	N/A	N/A	N/A	N/A	**0.006**	N/A	N/A
Log(Density) = s(Lat)	317.92	59.19	0	2.112	0.079	**0.037**	N/A	N/A	N/A	N/A	N/A	N/A	N/A
Log(Density) = s(NPP)	318.16	59.43	0	2.116	0.081	N/A	N/A	N/A	N/A	N/A	N/A	N/A	**0.031**
Log(Density) = s(Z)	323.52	64.79	0	2.255	0.003	N/A	N/A	N/A	N/A	0.262	N/A	N/A	N/A
Log(Density) = s(Ox)	323.53	64.8	0	2.245	0.036	N/A	N/A	0.336	N/A	N/A	N/A	N/A	N/A
Log(Density) = s(Sub)	324.81	66.08	0	2.288	0.000	N/A	N/A	N/A	N/A	N/A	N/A	0.934	N/A

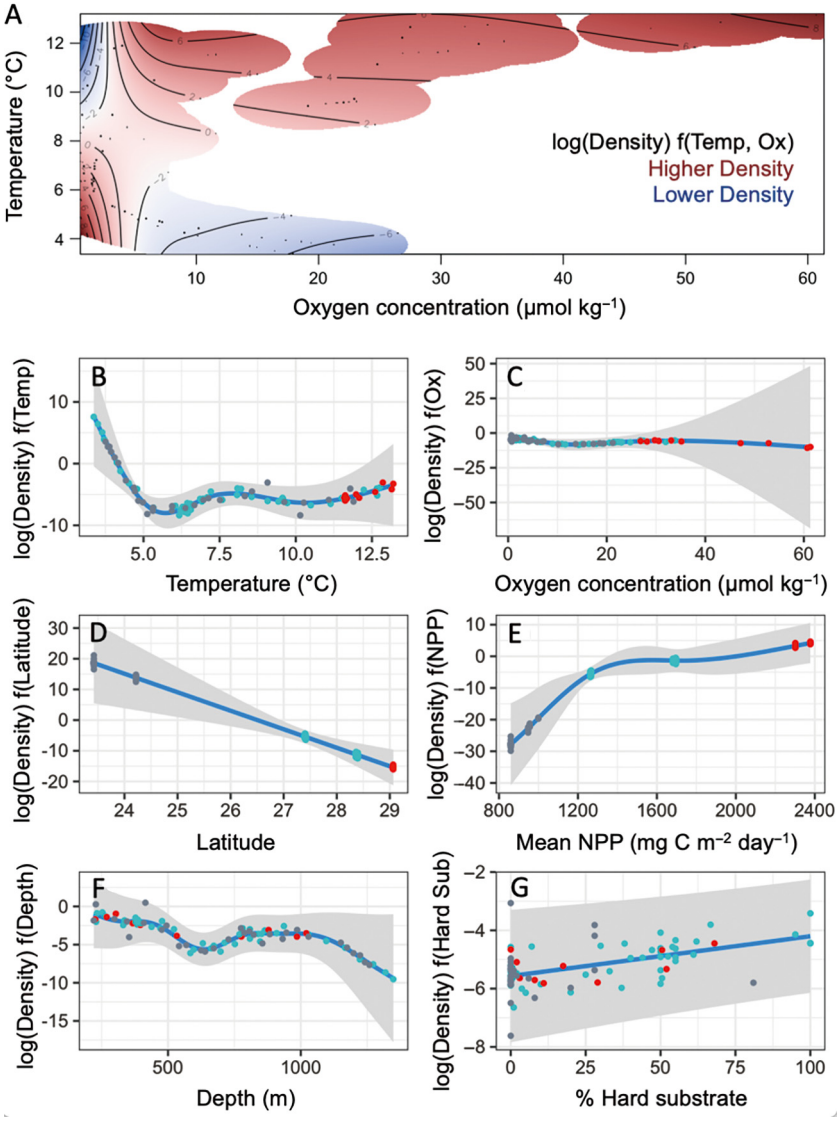

Fig. 5. Component plots for the highest ranked generalized additive model explaining variance in deep-sea demersal fish density in the Gulf of California. The model that included temperature and oxygen as main effects as well as an interaction between temperature and oxygen, latitude, mean net primary production (NPP), depth, and percent hard substrate could explain 75% of the observed variance in fish community density. (A) Fish density as a function of temperature and oxygen combined; blue: lower fish densities; red: higher densities; white: temperature–oxygen combinations not encountered during this study. For the lower 6 component plots (B–G) showing fish density as a function of environmental covariates, the blue line represents the expected value with a confidence interval shown in gray, and points represent partial residuals for each of the 88 transects, colored by location (red: northern, turquoise: central, gray: southern Gulf)

mean NPP, POC flux, depth and percent hard substrate were not found to be significant predictors (Table 4). Oxygen concentration was ranked as the most important variable for explaining variance in fish diversity (weight = 0.99), followed by latitude (weight = 0.77), and then POC flux, temperature, depth, mean NPP, and percent hard substrate, which all had variable importance weights below 0.31.

Since both fish density and diversity showed nonlinear relationships with oxygen and exhibited threshold responses, we used a segmented regression model to identify the oxygen concentration under which strong changes in fish density and diversity occurred. In both cases, the segmented regression models identified statistically significant thresholds ($p = 0.05$ for density and $p < 0.001$ for diversity). The oxygen threshold for diversity (7 ± 1 µmol kg^{-1}) was twice as high as the threshold for density (3 ± 1 µmol kg^{-1}); below these oxygen thresholds, fish density and diversity sharply declined (Fig. 7).

3.4. Demersal fish tolerance to severe hypoxia

Conditions were suboxic (<5 µmol kg^{-1}) for nearly half (43/88) of the transects conducted. Despite these severely hypoxic conditions, demersal fish were observed during 87 of 88 transects. No fish were observed along only one transect located at an intermediate depth (354 m) off Cabo Pulmo (Dive 738), where conditions were nearly anoxic (O_2 = 0.74 µmol kg^{-1}) and relatively warm (10.15°C). More than one fish species was present in 90% of transects. The highest fish density (3.26 fish m^{-2}) was observed during Dive 737 in the Cerralvo Trough at 774 m, under cold (5.94°C) and severely hypoxic (O_2 = 1.61 µmol kg^{-1}) conditions. Nearby transects also had fish densities ~4 times higher (0.46 fish m^{-2}) than the average fish density observed across other transects (0.11 fish m^{-2}), showing that the Cerralvo Trough supports high fish densities despite the presence of severely hypoxic conditions.

The ophidiid *C. emmelas* and the scyliorhinid *C. cephalus* consistently occurred under the most extreme hypoxic conditions encountered during the study. Other species were also present in suboxic communities, including *D. spinosus* and *N. liolepis*, but they were rarer and their distribution extended

Table 4. Generalized additive models evaluated for assessing the relationship between environmental variables and demersal fish diversity (H'_{ln}) across 88 transects in the Gulf of California. See Table 3 for further details

Equation	AIC_C	ΔAIC_C	Weight	GCV	R^2 (adj)	p							
						Lat	T	Ox	T,Ox	Z	POC	Sub	NPP
Diversity (H'_{ln}) = s(Lat) + s(Ox)	69.2	0	0.342	0.123	0.573	**0.018**	N/A	**<0.001**	N/A	N/A	N/A	N/A	N/A
Diversity (H'_{ln}) = s(Lat) + s(T) + s(Ox)	71.18	1.98	0.127	0.125	0.570	**0.024**	0.452	**<0.001**	N/A	N/A	N/A	N/A	N/A
Diversity (H'_{ln}) = s(Lat) + ti(T) + ti(Ox) + ti(T,Ox)	71.27	2.07	0.121	0.126	0.558	0.071	0.226	**<0.001**	0.314	N/A	N/A	N/A	N/A
Diversity (H'_{ln}) = s(Ox) + s(NPP)	71.9	2.69	0.089	0.126	0.564	N/A	N/A	**<0.001**	N/A	N/A	N/A	N/A	0.059
Diversity (H'_{ln}) = s(Lat) + ti(T) + ti(Ox) + ti(T,Ox) + s(Sub)	72.59	3.38	0.063	0.127	0.559	**0.041**	0.138	**<0.001**	0.398	N/A	N/A	0.211	N/A
Diversity (H'_{ln}) = s(Lat) + ti(T) + ti(Ox) + ti(T,Ox) + s(Z)	72.82	3.62	0.056	0.128	0.556	0.056	0.135	**<0.001**	0.569	0.313	N/A	N/A	N/A
Diversity (H'_{ln}) = s(Lat) + s(Ox) + s(NPP)	73.33	4.12	0.043	0.126	0.581	0.281	N/A	**<0.001**	N/A	N/A	N/A	N/A	0.215
Diversity (H'_{ln}) = s(Lat) + s(T) + s(Ox) + s(Z)	73.36	4.16	0.043	0.128	0.563	**0.022**	0.392	**<0.001**	N/A	0.559	N/A	N/A	N/A
Diversity (H'_{ln}) = s(Lat) + s(T) + s(Ox) + s(Sub)	73.5	4.3	0.04	0.128	0.563	**0.020**	0.333	**<0.001**	N/A	N/A	N/A	0.446	N/A
Diversity (H'_{ln}) = s(Lat) + ti(T) + ti(Ox) + ti(T,Ox) + s(NPP)	75.07	5.86	0.018	0.129	0.570	0.296	0.248	**<0.001**	0.363	N/A	N/A	N/A	0.697
Diversity (H'_{ln}) = s(Lat) + s(T) + s(Ox) + s(NPP)	75.14	5.94	0.018	0.128	0.582	0.300	0.372	**<0.001**	N/A	N/A	N/A	N/A	0.738
Diversity (H'_{ln}) = s(Lat) + ti(T) + ti(Ox) + ti(T,Ox) + s(Z) + s(Sub)	75.51	6.31	0.015	0.130	0.558	0.120	0.080	**<0.001**	0.239	0.448	N/A	0.356	N/A
Diversity (H'_{ln}) = s(Ox)	76.25	7.05	0.01	0.134	0.517	N/A	N/A	**<0.001**	N/A	N/A	N/A	N/A	N/A
Diversity (H'_{ln}) = s(Lat) + ti(T) + ti(Ox) + ti(T,Ox) + s(Z) + s(POC) + s(Sub)	76.94	7.74	0.007	0.131	0.570	0.155	0.093	**0.002**	0.299	0.278	0.319	0.136	N/A
Diversity (H'_{ln}) = s(Lat) + s(T) + s(Ox) + s(Z) + s(POC) + s(Sub)	77.86	8.66	0.004	0.131	0.571	**0.035**	0.111	**<0.001**	N/A	0.255	0.301	0.139	N/A
Diversity (H'_{ln}) = s(Lat) + s(T) + s(Ox) + s(Z) + s(Sub) + s(NPP)	79.66	10.46	0.002	0.131	0.590	0.252	0.065	**<0.001**	N/A	0.262	N/A	0.290	0.523
Diversity (H'_{ln}) = s(Lat) + ti(T) + ti(Ox) + ti(T,Ox) + s(Z) + s(Sub) + s(NPP)	79.92	10.72	0.002	0.131	0.591	0.109	0.108	**<0.001**	0.296	0.278	N/A	0.260	0.131
Diversity (H'_{ln}) = s(Lat) + ti(T) + ti(Ox) + ti(T,Ox) + s(Z) + s(POC) + s(Sub) + s(NPP)	82.5	13.3	0	0.134	0.586	0.312	0.328	**<0.001**	0.554	0.571	0.790	0.244	0.576
Diversity (H'_{ln}) = s(Lat) + s(T) + s(Ox) + s(Z) + s(POC) + s(Sub) + s(NPP)	83.06	13.86	0	0.135	0.586	0.280	0.193	**<0.001**	N/A	0.449	0.938	0.288	0.551
Diversity (H'_{ln}) = s(POC)	89.81	20.61	0	0.156	0.449	N/A	N/A	N/A	N/A	N/A	**<0.001**	N/A	N/A
Diversity (H'_{ln}) = s(T)	97.44	28.24	0	0.170	0.393	N/A	**<0.001**	N/A	N/A	N/A	N/A	N/A	N/A
Diversity (H'_{ln}) = s(Z)	102.27	33.07	0	0.179	0.368	N/A	N/A	N/A	N/A	**<0.001**	N/A	N/A	N/A
Diversity (H'_{ln}) = s(Lat)	131.32	62.11	0	0.253	0.053	0.171	N/A	N/A	N/A	N/A	N/A	N/A	N/A
Diversity (H'_{ln}) = s(Sub)	134.21	65.01	0	0.262	0.000	N/A	N/A	N/A	N/A	N/A	N/A	0.702	N/A
Diversity (H'_{ln}) = s(NPP)	134.46	65.25	0	0.263	0.000	N/A	N/A	N/A	N/A	N/A	N/A	N/A	0.850

into habitats that were deeper and more oxygen-rich (Table 2). Therefore, suboxic environments in the Gulf do not exclude demersal fish, and under colder temperatures can even support very high fish densities.

3.5. Climate change projections for the Gulf of California seafloor

Under the RCP8.5 scenario, the Gulf seafloor is projected to experience warming to 3.4°C (mean increase 1.08 ± 1.07°C; Fig. 8A) by 2081–2100. The strongest warming will occur in the northern (2.85 ± 0.52°C), then central (0.87 ± 0.49°C), and finally southern (0.50 ± 0.68°C) regions of the Gulf. Most of the Gulf seafloor may additionally experience modest deoxygenation (mean −0.21 µmol kg^{-1}) by 2081–2100. However, with a standard deviation almost 16 times the mean, spatial variability in dissolved oxygen change is expected (Fig. 8B). Regionally, dissolved oxygen may decrease up to 11.55 µmol kg^{-1} at the northern tip of the Gulf near the mouth of the Colorado River but increase up to 15.85 µmol kg^{-1} in the Delfín Basin north of the Isla Ángel de la Guarda. The near-bottom dissolved oxy-

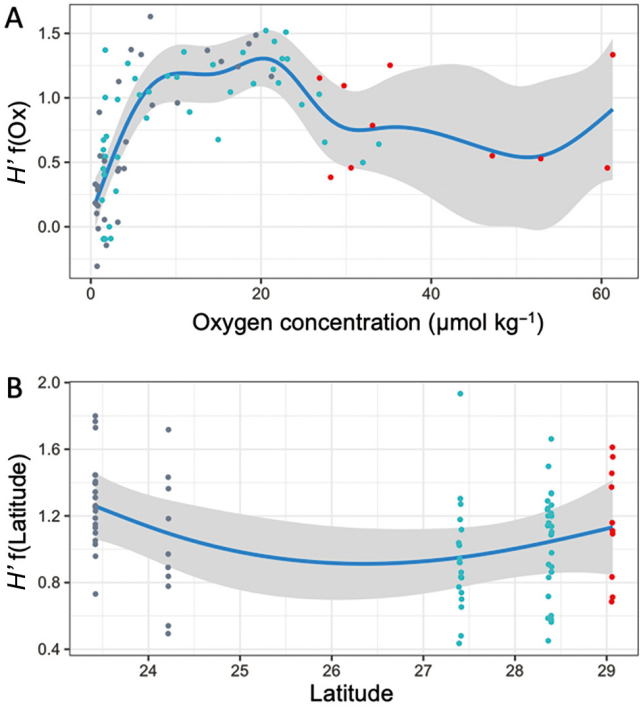

Fig. 6. Component plots for the highest ranked generalized additive model explaining variance in deep-sea demersal fish community diversity (H'_{ln}) in the Gulf of California. The model with (A) oxygen concentration and (B) latitude explained 57% of the observed variance. Blue line: expected value; gray shading: confidence interval; points: partial residuals for each of the 88 transects, colored by location (red: northern; turquoise: central; gray: southern Gulf)

gen concentration in the central and southern Gulf is expected to decline by 0.5 µmol kg^{-1} on average with relatively large standard deviations of approximately 2–3 times the mean.

By 2081–2100, oxygen levels across ~14% of the Gulf seafloor will be lower than 3 µmol kg^{-1}, the threshold below which fish density was observed to rapidly decrease (black contour line, Fig. 8B). Similarly, 16% of the Gulf seafloor is expected to have oxygen conditions below the threshold found to precede a rapid loss in fish diversity (red contour line, Fig. 8B). The percentage and coverage of these low-oxygen areas were found to be almost identical between the 1951–2000 and 2081–2100 projections, with little to no change in dissolved oxygen concentration (Fig. 8B). Despite the stability in oxygen conditions, temperatures in these low-oxygen areas are projected to increase by 0.42 ± 0.16°C (Fig. 8A).

4. DISCUSSION

This study provided the first descriptions of the deep-sea demersal fish community in the Gulf of California accompanied by genetic verification, environmental analyses, and climate change projections. We found that demersal fish community structure across the Gulf is highly correlated with variables that are expected to change with climate change (i.e. temperature, oxygen concentration, and primary production). Consequently, demersal fish

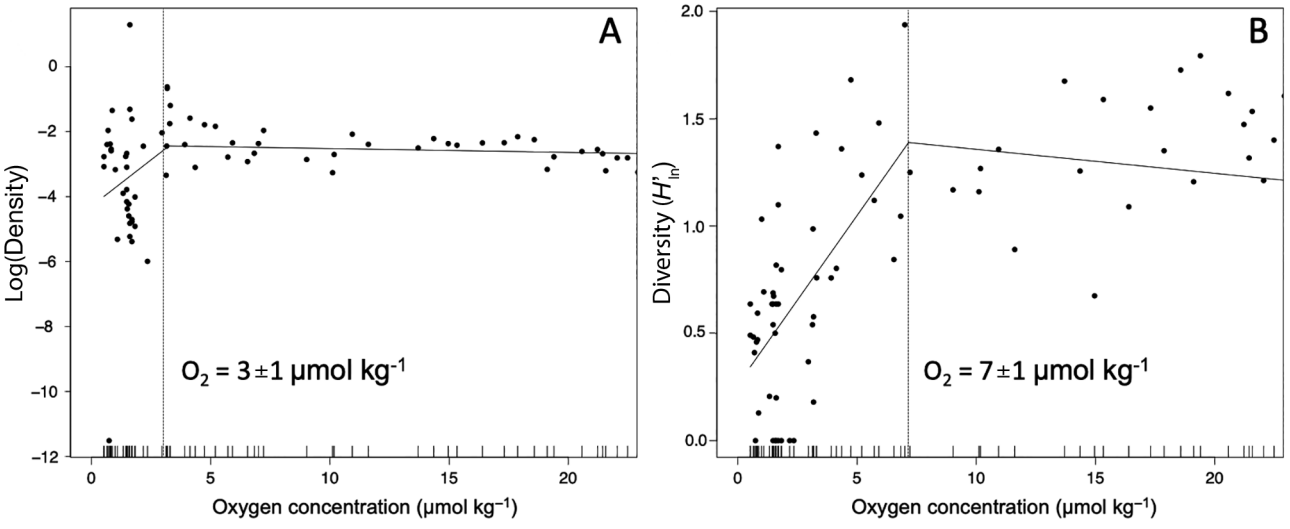

Fig. 7. Gulf of California deep-sea demersal fish (A) community density and (B) diversity (H'_{ln}) as a function of near-bottom oxygen concentration. A segmented regression model identified threshold responses of fish density (left) ($p = 0.05$) and fish diversity (right) ($p < 0.001$) with near-bottom oxygen concentration. Points: individual fish transects; dashed line: the oxygen threshold identified by the model (rounded to the nearest whole number). The rugplot shows the data distribution of oxygen conditions across the 88 transects

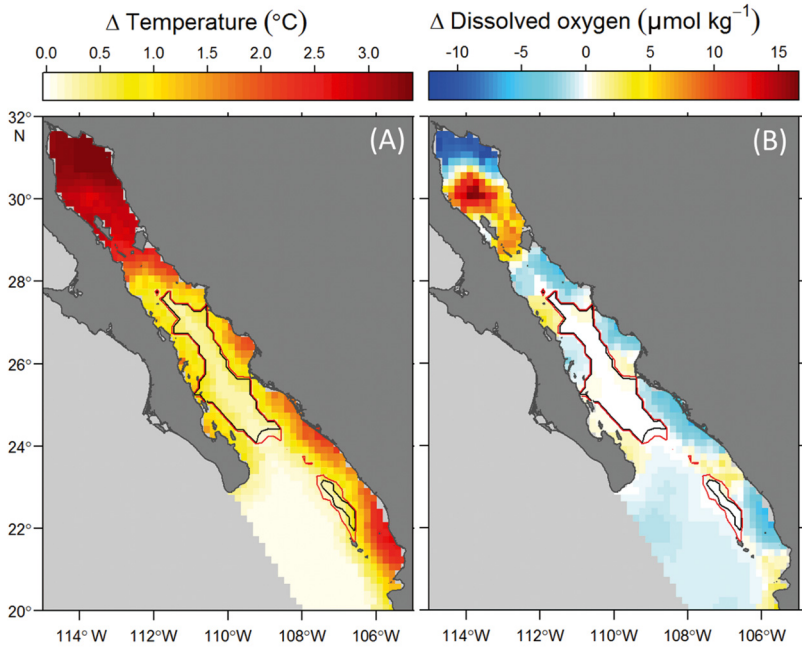

Fig. 8. Projected changes for average (A) seafloor temperature and (B) dissolved oxygen concentration between 1951–2000 and 2081–2100 using the MPI ESM-MR model output for an RCP8.5 scenario. Warm colors: increases; cool colors: decreases; white: no change. Black and red contour lines: dissolved oxygen concentration of 3.14 and 6.96 µmol kg^{-1} from 2081–2100, corresponding to the thresholds identified for decreasing fish density and diversity, respectively. The southern boundary of the northern Gulf of California is defined as 28° N latitude, the central Gulf is between 24° and 28° N, and the southern Gulf is between 20° and 24° N

communities in the Gulf are likely to be vulnerable to climate change impacts (Table 5).

Latitudinal differences previously described for the Gulf fish community indicated significant differences in larval assemblages between the northern and central Gulf, with the northern assemblage characterized by lower larval abundance and species richness (Ávalos-García et al. 2003). Overall fish species richness was reported as being twice as high in the south as in the north (Hastings et al. 2010). Our results (Figs. 3–6) lend support to some, but not all, of these latitudinal patterns. Deep-sea demersal fish community composition was related to latitude, with significant grouping by region and high dissimilarity across regions (Fig. 3). The first split in the MRT captured the strong difference in carbon flux between the northern and southern Gulf, which corresponds with differences in community composition (Fig. 4, Fig. S2). Our results for density trends with latitude were also consistent with previous studies, with fish densities higher in the southern than northern Gulf (Fig. 5).

In contrast to Hastings et al. (2010), we did not find large differences in fish diversity or species richness between the northern and southern Gulf. Previous studies on biogeographic patterns in the Gulf suggested regional differences in diversity may be driven partially by the high seasonal temperature variability in the northern Gulf (Roden 1964, Álvarez-Borrego 2010), which likely influences shallower communities more than the deep communities (>200 m) studied here. Furthermore, it is possible that the negative effects of hypoxia on diversity (Fig. 6) in the areas we studied masked latitudinal trends in diversity described by Hastings et al. (2010).

Depth (i.e. hydrostatic pressure) was not a significant explanatory factor for demersal fish diversity (Table 4), but was a predictor of trends in density (Table 3, Fig. 5) with density declining with increasing depth, and was a predictor of trends in community composition (Fig. 4). In areas like the deep Salsipuedes Basin, with relatively warm, well-oxygenated conditions, Parker (1964) noted virtually no stratification of macroinvertebrates. We similarly observed very limited zonation in the Salsipuedes Basin and found *Sebastes cortezi*, *Eptatretus* sp., and *Symphu-*

Table 5. Relative variable importance of the 3 community metrics examined in the study (deep-sea demersal fish community composition, density, and diversity). Environmental variables are ranked from 1 (most) to 7 (least) in terms of relative importance. For community composition, variable importance was determined by summing the total variance explained (R^2) by each individual variable in the multivariate regression tree with the smallest cross-validation relative error, which contained 17 splits. For density and diversity, variable importance was determined using variable importance weights (Burnham & Anderson 2002). POC: particulate organic carbon; NPP: net primary productivity

	Oxygen	Temperature	Latitude	POC Flux	Depth	% Hard substrate	Mean NPP
Community composition	1	5	6	2	4	3	7
Density	2[a]	1	3	7	5	6	4
Diversity (H'_{ln})	1	4	2	3	5	7	6

[a]For density, oxygen had high variable importance as an interactive effect with temperature

rus spp. occupying a broad depth range (~250–1000 m). Our results suggest that in margin communities with observable depth zonation, researchers should explore if other environmental covariates can explain the 'depth-related' patterns.

Consistent with our results for fish communities, oxygen levels appear to play a greater role than other environmental factors (depth, epibenthic temperature, sediment texture, and organic matter content) in explaining the density and diversity of molluscan communities in the Gulf (Zamorano et al. 2007). The threshold we report for oxygen (O_2 ~ 7 ± 1 µmol kg^{-1}) below which fish diversity declines rapidly is remarkably similar to that identified for diversity in Eastern Pacific macrofaunal communities (7.5 µmol kg^{-1}) (Sperling et al. 2016).

Our results suggest that fish diversity is a more sensitive metric to low-oxygen conditions than fish density. We hypothesize that this difference may be due to the following succession of hypoxia impacts. As oxygen concentrations decrease, hypoxia-intolerant fish species are excluded from severely hypoxic areas, resulting in altered community composition (Fig. 4) and decreased diversity (Fig. 6). These areas may then become food-rich refugia from predators, thereby supporting high densities of the few tolerant species. OMZ-adapted species often have lower metabolic rates (Levin 2003, Seibel 2011, Gallo & Levin 2016) than hypoxia-intolerant species, and thus may have lower food requirements, allowing for the environment to support such high densities. However, even the most hypoxia-tolerant species experience metabolic limitation under combinations of certain temperature and oxygen conditions, leading to a decline in densities when those conditions are encountered (Fig. 5). It should be noted that this study looked at density and not biomass, and it would be of interest to examine if fish biomass exhibits similar response patterns.

Our results indicate the importance of considering temperature and oxygen together when assessing habitat suitability for fish assemblages. For example, the only transect we sampled where fish were absent was relatively warm (10.15°C) and suboxic (O_2 = 0.74 µmol kg^{-1}). Since fish were observed in several transects with even lower oxygen levels (O_2 = 0.52–0.69 µmol kg^{-1}) but colder temperatures (7.1–9.0°C), it is likely that the increased metabolic demand in warmer waters (Deutsch et al. 2015) rendered this site unsuitable for even the most hypoxia-tolerant fish species. Similarly, mismatches between oxygen supply and metabolic demand have been implicated in the decreased abundance of the eelpout *Zoarces viviparous* as water temperatures warmed, though the oxygen conditions at that study site were much higher (Pörtner & Knust 2007).

Although benthic substrate was not found to be a dominant predictor of trends in fish community structure, we caution that this study was not designed to examine this factor in detail, and the transect design (in which multiple habitat types could be sampled by one transect) may weaken the signal. A more comprehensive design exploring habitat variation in relation to fish community structure may reveal stronger habitat-related patterns in the Gulf. Similarly, our metrics for food input (mean NPP and carbon flux) were based on satellite-derived estimates. More direct measures of food input and availability from water column or sediment trap samples could allow greater resolution between these food and fish patterns. Nevertheless, POC flux was associated with variation in the composition of fish communities (Fig. 4), and mean NPP was positively related to fish densities (Fig. 5).

4.1. Unique features of the Gulf fish community

A total of 77 demersal fish species have previously been described living under severely hypoxic conditions (O_2 < 22.5 µmol kg^{-1}) (Gallo & Levin 2016). This study adds an additional 18 species (Table 2), raising the number of demersal fish species globally known to live in OMZ conditions to 95 (Table S1 in Supplement 2). This number is likely conservative as many OMZ margins remain poorly studied, but still small compared to the global estimate (3000–4000) of species richness for deep-sea fishes (Koslow et al. 1997). Elevated hypoxia tolerance in the pelagic fish community has also been reported in the Gulf, with high species richness and abundance of larvae in severely hypoxic areas (Davies et al. 2015).

While many invertebrates are absent from the Gulf's severely hypoxic habitats, tolerant species commonly occur in the OMZ (Parker 1964, Zamorano et al. 2007). However, even hypoxia-tolerant galatheid crabs were never recorded at oxygen levels below ~2 µmol kg^{-1} (0.05 ml l^{-1}) in the Gulf (Hendrickx & Serrano 2014). In contrast, we observed several demersal fish species, including *Cherublemma emmelas*, *Cephalurus cephalus*, and *Dibranchus spinosus*, living in areas where oxygen content is below 2 µmol kg^{-1}, suggesting that fish in the Gulf may be more hypoxia-tolerant than most crustaceans. *C. emmelas* and *C. cephalus* have been proposed to be ligooxyphiles (low-oxygen specialists) (Gallo et al. 2019).

High-density aggregations of invertebrates are common features of OMZ habitats (Mullins et al. 1985, Levin 2003, Zamorano et al. 2007, Jeffreys et al. 2012) and we also observed high-density aggregations of fish, dominated by *C. emmelas*, within the OMZ. Fish densities were highest in the Cerralvo Trough (~3.26 fish m^{-2}, O_2 = 1.6 µmol kg^{-1}), where the local bathymetry may have additionally enhanced fish densities, but were also elevated off Cabo Pulmo (~0.24 fish m^{-2}, O_2 = 1.6 µmol kg^{-1}), suggesting the high-density feature may be related to the oxygen conditions. Off Hawai'i, submarine canyons were found to enhance the abundance of deep-sea demersal fish; however, this effect was offset when oxygen concentrations fell below ~30 µmol kg^{-1} (0.7 ml l^{-1}) (De Leo et al. 2012).

We observed midwater fish interacting oddly with the seafloor for as yet unknown reasons. At intermediate depths (~400–800 m) in the southern Gulf, bathylagids and myctophids rapidly swam down and crashed headfirst into the sediment, before swimming away. This behavior was most common in the nearly anoxic areas (O_2 < 1 µmol kg^{-1}). It is unclear if the fish were reacting to the ROV lights, feeding on the sediment, or were physiologically impaired by the near-anoxic conditions. These interactions were not observed in either the central or northern Gulf.

4.2. Study constraints

This study presents a snapshot of the deep-sea demersal fish community in the Gulf in late March 2015. However, the northern Gulf experiences significant seasonality, with shallow-water temperatures spanning 15°C between January and August (Parker 1964). Temporal oxygen variability has also been described for the deep Salsipuedes Basin (Álvarez-Borrego 1983) and the southern Gulf (Roden 1964). The abundance and distribution of midwater and larval fishes in the Gulf are known to vary interannually and seasonally (Moser et al. 1971, Ávalos-García et al. 2003, Sánchez-Velasco et al. 2009). Larvae of several demersal species included in this study (*Coelorinchus scaphopsis*, *Physiculus rastrelliger*, *C. emmelas*, *Pontinus* spp., *Bathycongrus macrurus*, and *Symphurus oligomerus*) showed seasonal and interannual changes in abundance in response to La Niña and El Niño events (Sánchez-Velasco et al. 2004). Whether the deep-sea demersal fish community also responds to pronounced environmental variability would be a valuable area of research in the future — our results suggest that environmental changes, particularly oxygen and temperature, could have large effects.

This study focused on adult fish that can easily be observed with the ROV. Consequently, we missed the early life stages. Studies on larval fish assemblages in the Gulf have found clear relationships between larval assemblages and oceanographic variables (Ávalos-García et al. 2003, Davies et al. 2015), and larvae of demersal fish are often captured and reported in these ichthyoplankton data sets (Moser et al. 1971). Understanding the influence of environmental variables on these early life stages is also important in determining how species will fare under climate change scenarios.

While we did not measure carbonate system parameters in this study, pH conditions are highly and positively correlated with oxygen conditions for the Gulf (Álvarez-Borrego 1983). Within the core of the OMZ, where oxygen values are lowest, low pH values (between 7.63 and 7.66) have been reported (Gaxiola-Castro et al. 1978). In the central and southern Gulf, the water becomes rapidly undersaturated with respect to calcite (300 m) and aragonite (70 m) (Gaxiola-Castro et al. 1978, Álvarez-Borrego 1983). Since oxygen and pH are highly correlated, we cannot state that the relationships found between fish community metrics and oxygen is not also influenced by carbonate system parameters, and encourage future studies to explore this relationship.

4.3. Implications for climate change impacts

Based on climate change projections for 2100, benthic ecosystems in the deep Gulf will likely experience larger changes in temperature than oxygen. The limited projected oxygen decline is somewhat surprising given that the spatial extent of suboxic areas is expected to be highly sensitive to climate-driven oxygen loss (Deutsch et al. 2011). This result may be due to model uncertainty and the difficulty of capturing small oxygen changes in areas already low in dissolved oxygen. Despite the limited oxygen decline predicted by the climate model, fish communities may still experience oxygen stress, as warming increases metabolic rates and oxygen demand (Pörtner et al. 2017). Regional differences in warming are predicted, with the northern Gulf expected to experience the most warming, followed by the central and southern Gulf. The eastern Gulf may also experience greater warming and oxygen loss than the western Gulf (Fig. 8). Based on our results, communities in the central Gulf may be especially vulnerable to climate-driven metabolic constraints. Currently, oxygen conditions for ~41% of the seafloor in the central Gulf

are lower than the threshold found in this study to correlate with decreases in fish diversity (O_2 ~ 7 µmol kg^{-1}), and the central Gulf seafloor is projected to warm by 0.87 ± 0.49°C by 2100.

Examining the temperature and oxygen niches of species may offer an opportunity to explore species-specific vulnerabilities to climate change and possible metabolic limits on species distributions based on combined temperature and oxygen stress. *C. scaphopsis*, a shallow-water (220–550 m) grenadier common in the northern and upper central Gulf, is absent in the southern and lower central Gulf where severely hypoxic conditions (O_2 < 10 µmol kg^{-1}) are present in shallow (200–500 m) areas. If *C. scaphopsis* is restricted to higher oxygen habitats due to a high metabolism, the combination of warming and oxygen loss projected for the northern and central Gulf may result in significant habitat compression for this species. The 'metabolic index' has been proposed as a mechanistic framework for understanding marine species distributions, with contemporary distributions limited to areas where the environmental oxygen supply is at least 2–5 times greater than the animal's resting metabolic oxygen demand (Deutsch et al. 2015). Relating projected changes in the metabolic index for the Gulf with current environmental niches for demersal fish species may allow for valuable insight into organismal and ecosystem vulnerabilities to climate change.

5. CONCLUSIONS

Oxygen and temperature are highly correlated with trends in deep-sea demersal fish community structure in the Gulf of California. Consequently, climate changes with resulting impacts on the oxygen and temperature regimes in the Gulf will likely lead to altered demersal fish community composition, density, and diversity. Near-bottom oxygen is the strongest factor explaining variation in demersal fish community diversity and composition, while temperature has more explanatory power for trends in density. Warming is projected to be more pronounced for the Gulf than deoxygenation, and the influence of warming temperatures on metabolic rates may lead to additional oxygen stress for fish communities. Additional factors linked to ocean acidification were not examined here, but could contribute to cumulative stress on fishes. We found that several demersal fish species exhibited remarkable hypoxia tolerance; however, these species currently lack economic value, while important commercial species, such as *Sebastes macdonaldi*, are excluded from severely hypoxic areas. Coupled observations of community trends across natural gradients with climate model projections provided a valuable tool for exploring ecosystem vulnerabilities to climate change. Additional laboratory and geochemical proxy approaches may help to verify the environment–community relationships documented here and generate further mechanistic understanding.

Acknowledgements. The study was supported by the David and Lucile Packard Foundation and MBARI project 901007. We thank Ron Burton for providing the facilities and support for the sequencing work, H. J. Walker, Phil Hastings, and Ben Frable of the SIO Fish Collections for help with identifying collected specimens, and John Hyde of NOAA SWFSC for help sequencing and identifying observed and collected rockfish. We also thank the terrific pilots and technicians of the ROV 'Doc Ricketts', Knute Brekke, Randy Prickett, Bryan Touryan-Schaefer, Mark Talkovic, and Ben Erwin, and the crew and scientific party of the R/V 'Western Flyer'. We also thank R. Burton, A. G. Salvanes, B. Semmens, D. Victor, and 2 anonymous reviewers for feedback on the manuscript. We acknowledge funding from the Ministry of Science and Technology, Taiwan (MOST 108-2611-M-002-001) to C.L.W. N.D.G. was supported by National Science Foundation Graduate Research Fellowship under grant no. DGE-1144086. Any opinion, findings, and conclusions or recommendations expressed in this material are those of the authors and do not necessarily reflect the views of the National Science Foundation.

LITERATURE CITED

Álvarez-Borrego S (1983) Gulf of California. In: Ketchum BH (ed) Estuaries and enclosed seas. Elsevier, Amsterdam, p 427–449

Álvarez-Borrego S (2010) Physical, chemical and biological oceanography of the Gulf of California. In: Brusca RC (ed) The Gulf of California: biodiversity and conservation. University of Arizona Press, Tucson, AZ, p 24–48

Ávalos-García C, Sánchez-Velasco L, Shirasago B (2003) Larval fish assemblages in the Gulf of California and their relation to hydrographic variability (Autumn 1997-Summer 1998). Bull Mar Sci 72:63–76

Ayma A, Aguzzi J, Canals M, Lastras G, Bahamon N, Mecho A, Company JB (2016) Comparison between ROV video and Agassiz trawl methods for sampling deep water fauna of submarine canyons in the northwestern Mediterranean Sea with observations on behavioural reactions of target species. Deep Sea Res I 114:149–159

Bartoń K (2019) MuMIn: multi-model inference. R package version 1.43.6

Bivand R, Lewin-Koh N (2017) maptools: tools for reading and handling spatial objects. R package version 0.9-2

Bivand RS, Pebesma E, Gomez-Rubio V (2013) Applied spatial data analysis with R. Springer, New York, NY

Bopp L, Resplandy L, Orr JC, Doney SC and others (2013) Multiple stressors of ocean ecosystems in the 21st century: projections with CMIP5 models. Biogeosciences 10: 6225–6245

Bradbury MG (1999) A review of the fish genus *Dibranchus* with descriptions of new species and a new genus,

Solocisquama (Lophiiformes, Ogcocephalidae). Proc Calif Acad Sci 51:259–310

Breheny P, Burchett W (2017) visreg: visualization of regression models. R package version 2.4-1

Breitburg D, Levin LA, Oschlies A, Grégoire M and others (2018) Declining oxygen in the global ocean and coastal waters. Science 359:eaam7240

Brewer GD (1973) Midwater fishes from the Gulf of California and the adjacent eastern tropical Pacific. Contrib Sci 242:1–47

Brown A, Thatje S (2014) Explaining bathymetric diversity patterns in marine benthic invertebrates and demersal fishes: physiological contributions to adaptations of life at depth. Biol Rev Camb Philos Soc 89:406–426

Brusca RC, Hendrickx ME (2010) Invertebrate biodiversity and conservation in the Gulf of California. In: Brusca RC (ed) The Gulf of California: biodiversity and conservation. University of Arizona Press, Tucson, AZ, p 72–95

Burnham KP, Anderson DR (2002) Model selection and multimodel inference: a practical information-theoretic approach, 2nd edn. Springer-Verlag, New York, NY

Carney RS (2005) Zonation of deep biota on continental margins. Oceanogr Mar Biol Annu Rev 43:211–278

Clarke A, Gaston KJ (2006) Climate, energy and diversity. Proc R Soc B 273:2257–2266

Clarke KR, Gorley RN (2006) PRIMER v6: user manual/tutorial. PRIMER-E, Plymouth

Davies SM, Sánchez-Velasco L, Beier E, Godínez VM, Barton ED, Tamayo A (2015) Three-dimensional distribution of larval fish habitats in the shallow oxygen minimum zone in the eastern tropical Pacific Ocean off Mexico. Deep Sea Res I 101:118–129

De la Cruz-Agüero J, Galván-Magaña F (1992) Peces mesopelágicos de la costa occidental de Baja California Sur y del Golfo de California. An Inst Cienc Mar Limnol Unv Nac Auton Mex 19:25–31

De Leo FC, Drazen JC, Vetter EW, Rowden AA, Smith CR (2012) The effects of submarine canyons and the oxygen minimum zone on deep-sea fish assemblages off Hawai'i. Deep Sea Res I 64:54–70

De'ath G (2002) Multivariate regression trees: a new technique for modeling species–environment relationships. Ecology 83:1105–1117

De'ath G (2014) mvpart: multivariate partitioning. R package version 1.6-2. https://CRAN.R-project.org/src/contrib/Archive/mvpart

Del Moral-Flores LF, González-Acosta AF, Espinosa-Pérez H, Ruiz-Campos G, Castro-Aguirre JL (2013) Annotated checklist of the ichthyofauna from the islands of the Gulf of California, with comments on its zoogeographic affinities. Rev Mex Biodivers 84:184–214

Deutsch C, Brix H, Ito T, Frenzel H, Thompson L (2011) Climate-forced variability of ocean hypoxia. Science 333: 336–339

Deutsch C, Ferrel A, Seibel B, Pörtner HO, Huey RB (2015) Climate change tightens a metabolic constraint on marine habitats. Science 348:1132–1135

Espinosa-Carreón TL, Escobedo-Urías D (2017) South region of the Gulf of California large marine ecosystem upwelling, fluxes of CO_2 and nutrients. Environ Dev 22: 42–51

Fischer W, Krupp F, Schneider W, Sommer C, Carpenter KE, Niem VH (1995a) Guia FAO para la identificacion de especies para los fines de la pesca. Pacifico centro-oriental, Vol 2: Vertebrados, Parte 1. FAO, Rome

Fischer W, Krupp F, Schneider W, Sommer C, Carpenter KE, Niem VH (1995b) Guia FAO para la identificacion de especies para los fines de la pesca. Pacifico centro-oriental, Vol 3. Vertebrados, Parte 2. FAO, Rome

Gallo ND, Levin LA (2016) Fish ecology and evolution in the world's oxygen minimum zones and implications of ocean deoxygenation. Adv Mar Biol 74:117–198

Gallo ND, Levin LA, Beckwith M, Barry JP (2019) Home sweet suboxic home: remarkable hypoxia tolerance in two demersal fish species in the Gulf of California. Ecology 100:e02539

Gaxiola-Castro G, Álvarez-Borrego S, Schwartzlose RA (1978) Sistema del bióxido de carbano en el Golfo de California. Cienc Mar 5:25–40

Giorgetta MA, Jungclaus J, Reick CH, Legutke S and others (2013) Climate and carbon cycle changes from 1850 to 2100 in MPI-ESM simulations for the Coupled Model Intercomparison Project phase 5. J Adv Model Earth Syst 5:572–597

Gräler B, Pebesma E, Heuvelink G (2016) Spatio-temporal interpolation using gstat. R J 8:204–218

Hastie TJ, Tibshirani RJ (1986) Generalized additive models. Stat Sci 1:297–318

Hastings PA, Findley LT, Van der Heiden AM (2010) Fishes of the Gulf of California. In: Brusca RC (ed) The Gulf of California: biodiversity and conservation. University of Arizona Press, Tucson, AZ, p 96–118

Hendrickx ME, Serrano D (2014) Effects of the oxygen minimum zone on squat lobster distributions in the Gulf of California, Mexico. Cent Eur J Biol 9:92–103

Hijmans RJ (2016) raster: geographic data analysis and modeling. R package version 2.5-8

IPCC (2019) Summary for policymakers. In: Pörtner HO, Roberts DC, Masson-Delmotte V, Zhai P and others (eds) IPCC Special Report on the ocean and cryosphere in a changing climate. Cambridge University Press, Cambridge

Jeffreys RM, Levin LA, Lamont PA, Woulds C and others (2012) Living on the edge: single-species dominance at the Pakistan oxygen minimum zone boundary. Mar Ecol Prog Ser 470:79–99

Johannesen E, Høines AS, Dolgov AV, Fossheim M (2012) Demersal fish assemblages and spatial diversity patterns in the Arctic-Atlantic transition zone in the Barents Sea. PLOS ONE 7:e34924

Keller AA, Ciannelli L, Wakefield WW, Simon V, Barth JA, Pierce SD (2015) Occurrence of demersal fishes in relation to near-bottom oxygen levels within the California Current large marine ecosystem. Fish Oceanogr 24:162–176

Keller AA, Ciannelli L, Wakefield WW, Simon V, Barth JA, Pierce SD (2017) Species-specific responses of demersal fish to near-bottom oxygen levels within the California Current large marine ecosystems. Mar Ecol Prog Ser 568: 151–173

Koslow JA, Williams A, Paxton JR (1997) How many demersal fish species in the deep sea? A test of a method to extrapolate from local to global biodiversity. Biodivers Conserv 6:1523–1532

Lavenberg RJ, Fitch JE (1966) Annotated list of the fishes collected by mid-water trawl in the Gulf of California, March–April 1964. Calif Fish Game 52:92–110

Levin LA (2003) Oxygen minimum zone benthos: adaptation and community response to hypoxia. Oceanogr Mar Biol Annu Rev 41:1–45

Levin LA, Sibuet M (2012) Understanding continental margin biodiversity: a new imperative. Annu Rev Mar Sci 4:79–112

López-Martínez J, Acevedo-Cervantes A, Herrera-Valdivia E, Rodríguez-Romero J, Palacios-Salgado DS (2012) Composición taxonómica y aspectos zoogeográficos de peces

de profundidad (90–540 m) del Golfo de California, México. Rev Biol Trop 60:347–360
Lutz MJ, Caldeira K, Dunbar RB, Behrenfeld MJ (2007) Seasonal rhythms of net primary production and particulate organic carbon flux to depth describe the efficiency of biological pump in the global ocean. J Geophys Res 112:C10011
McClatchie S, Goericke R, Cosgrove R, Auad G, Vetter R (2010) Oxygen in the Southern California Bight: multidecadal trends and implications for demersal fisheries. Geophys Res Lett 37:L19602
Mejía-Mercado BE, Balart-Páez E, Sosa-Nishizaki O, Hinojoso-Corona A (2014) Registros de especies ícticas (Myxini, Chondrichthyes, y Actinopterygii). In: Mejía Mercado BE, Hinojosa Corona A, Hendrickx ME (eds) Explorando el mar profundo del Golfo de California: 2008–2014. CICESE, Ensenada, p 206–226
Mora C, Wei CL, Rollo A, Amaro T and others (2013) Biotic and human vulnerability to projected changes in ocean biogeochemistry over the 21st century. PLOS Biol 11: e1001682
Moser HG, Ahlstrom EH, Kramer D, Stevens EG (1971) Distribution and abundance of fish larvae in the Gulf of California. CCOFI Rep 17:112–128
Muggeo VMR (2008) segmented: an R package to fit regression models with broken-line relationships. R News 8: 20–25
Mullins HT, Thompson JB, McDougall K, Vercoutere TL (1985) Oxygen-minimum zone edge effects: evidence from the central California coastal upwelling system. Geology 13:491–494
Nielsen JG, Cohen DM, Markle DF, Robins CR (1999) Ophidiiform fishes of the world (Order Ophidiiformes): an annotated and illustrated catalogue of pearlfishes, cusk-eels, brotulas and other ophidiiform fishes known to date. FAO Fish Synop 125:1–190
Oksanen J, Blanchet FG, Friendly M, Kindt R and others (2017) vegan: community ecology package. R package version 2.4-4
Ouellette MH, Legendre P (2013) MVPARTwrap: additional features for package mvpart. R package version 0.1-9.2. https://CRAN.R-project.org/src/contrib/Archive/MVPARTwrap
Parker RH (1964) Zoogeography and ecology of macroinvertebrates of Gulf of California and continental slope of western Mexico. Mem Am Assoc Pet Geol 3:331–376
Pörtner HO, Knust R (2007) Climate change affects marine fishes through the oxygen limitation of thermal tolerance. Science 315:95–97
Pörtner HO, Karl DM, Boyd PW, Cheung WWL and others (2014) Ocean systems. In: Field CB, Barros VR, Dokken DJ, Mach KJ and others (eds) Climate change 2014: impacts, adaptation, and vulnerability. Part A: global and sectoral aspects. Contribution of Working Group II to the Fifth Assessment Report of the Intergovernmental Panel on Climate Change. Cambridge University Press, Cambridge, p 411–484
Pörtner HO, Bock C, Mark KC (2017) Oxygen- and capacity-limited thermal tolerance: bridging ecology and physiology. J Exp Biol 220:2685–2696
R Core Team (2019) R: a language and environment for statistical computing. R Foundation for Statistical Computing, Vienna
Robison BH (1972) Distribution of the midwater fishes of the Gulf of California. Copeia 1972:448–461
Roden GI (1964) Oceanographic aspects of the Gulf of California. Mem Am Assoc Pet Geol 3:30–58
Sánchez-Velasco L, Ávalos-García C, Renteria-Cano M, Shirasago B (2004) Fish larvae abundance and distribution in the central Gulf of California during strong environmental changes (1997–1998 El Niño and 1998–1999 La Niña). Deep Sea Res II 51:711–722
Sánchez-Velasco L, Lavín MF, Peguero-Icaza M, León-Chávez CA and others (2009) Seasonal changes in larval fish assemblages in a semi-enclosed sea (Gulf of California). Cont Shelf Res 29:1697–1710
Schlining BM, Stout NJ (2006) MBARI's video annotation and reference system. In: Proceedings of the Marine Technology Society/Institute of Electrical and Electronics Engineers Oceans Conference, Boston, MA, p 1–5
Seibel BA (2011) Critical oxygen levels and metabolic suppression in oceanic oxygen minimum zones. J Exp Biol 214:326–336
Snelgrove PVR, Soetaert K, Solan M, Thrush S and others (2018) Global carbon cycling on a heterogenous seafloor. Trends Ecol Evol 33:96–105
Sperling EA, Frieder CA, Levin LA (2016) Biodiversity response to natural gradients of multiple stressors on continental margins. Proc R Soc B 283:20160637
Springer S (1979) A revision of the catsharks, Family Scyliorhinidae. NOAA Tech Rep NMFS Circular 422
Sverdrup HU (1941) The Gulf of California: preliminary discussion on the cruise of the EW Scripps in February and March 1939. In: Proc 6th Pacific Sci Congr 3: 161–166
Sweetman AK, Thurber AR, Smith CR, Levin LA and others (2017) Major impacts of climate change on deep-sea benthic ecosystems. Elem Sci Anth 5:4
Thomson DA, Eger WH (1966) Guide to the families of the common fishes of the Gulf of California. University of Arizona Press, Tucson, AZ
Thomson DA, Findley LT, Kerstitch AN (2000) Reef fishes of the Sea of Cortez: the rocky-shore fishes of the Gulf of California. University of Texas Press, Austin, TX
Vaquer-Sunyer R, Duarte CM (2008) Thresholds of hypoxia for marine biodiversity. Proc Natl Acad Sci USA 105: 15452–15457
Walker BW (1960) The distribution and affinities of the marine fish fauna of the Gulf of California. Syst Zool 9: 123–133
Walker HJ, Rosenblatt RH (1988) Pacific toadfishes of the Genus *Porichthys* (Batrachoididae) with descriptions of three new species. Copeia 1988:887–904
Walsh PS, Metzger DA, Higuchi R (2013) Chelex 100 as a medium for simple extraction of DNA for PCR-based typing from forensic material. Biotechniques 54:134–139
Wood SN (2017) Generalized additive models: an introduction with R. CRC Press, Boca Raton, FL
Zamorano P, Hendrickx ME, Toledano-Granados A (2007) Distribution and ecology of deep-water mollusks from the continental slope, southeastern Gulf of California, Mexico. Mar Biol 150:883–892
Zamorano P, Hendrickx ME, Méndez N, Goméz S and others (2014) La exploración de las aguas profundas del Pacífico mexicano: el proyecto TALUD. In: Pfeng AL, Peters Recagno EM (eds) La Frontera Final: El Océano Profundo. Instituto Nacional de Ecología, Secretaría del Medio Ambiente y Recursos Naturales, Mexico City, p 107–151

Editorial responsibility: Elliott Hazen, Pacific Grove, California, USA

Submitted: October 9, 2019; Accepted: January 17, 2020
Proofs received from author(s): February 24 , 2020